PETROLOGY

of the

TERTIARY ANCHOR CANYON STOCK,

MAGDALENA MOUNTAINS, CENTRAL NEW MEXICO

by

David E. Park

THESIS

Submitted to the faculty of the
New Mexico Institute of Mining and Technology
in partial fulfillment of the requirements for
the degree of Master of Science
in Geology

New Mexico Institute of Mining and Technology
Socorro, New Mexico

May, 1971

The Magdalena Mountains looking south southeast with Anchor Canyon in the foreground.

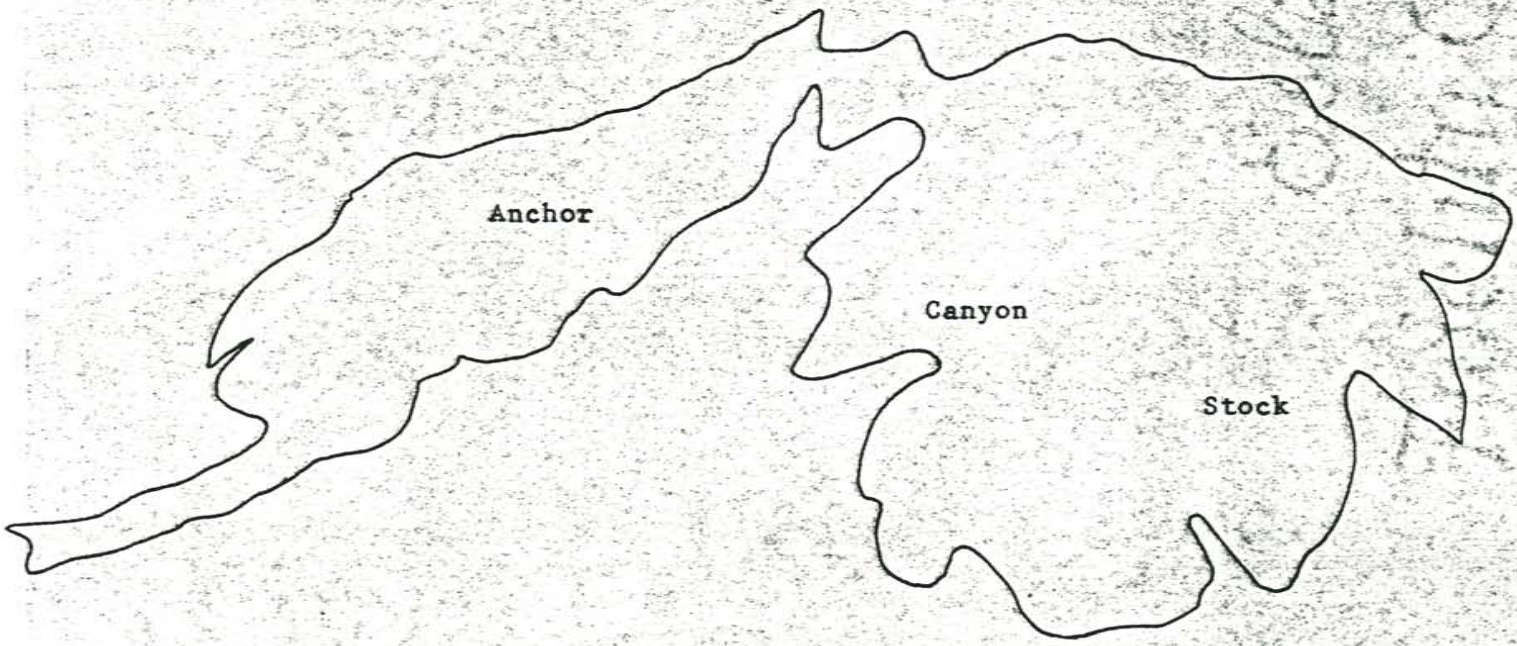

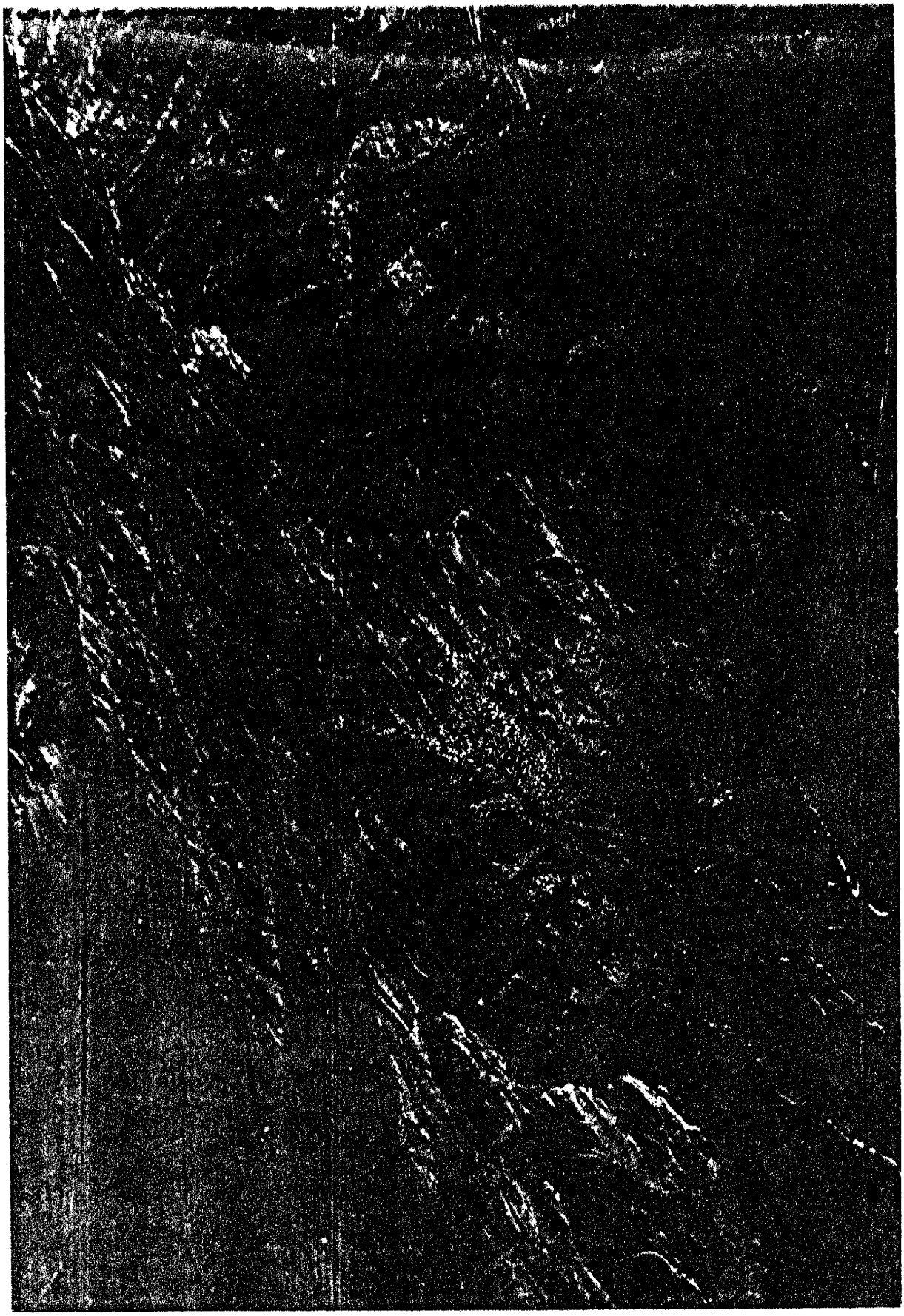

ABSTRACT

The Tertiary Anchor Canyon stock comprises a 2½-square-mile area at the northern end of the Magdalena Mountains. It intrudes a Precambrian basement complex consisting of quartzite, felsite, and granite and also Paleozoic limestones, sandstones, and shales. A K/Ar age of 28.3 m.y. was obtained from the pluton.

The stock has been divided into four rock types: I, augite-quartz monzonite; II, hornblende-biotite-quartz monzonite; III, augite granite; and IV, hornblende-biotite granite. The contacts between rock types are gradational. Modal data show a systematic compositional variation with elevation and east-west direction. Orthoclase and quartz increase with higher elevation while plagioclase and mafics decrease. Geochemical data, except for K_2O, Al_2O_3 and Rb, follow normal fractionation trends. The variation is best explained by the gravitational differentiation of a crystal-rich magma during ascent from the lower crust and by rise and concentration of the volatile constituents after emplacement. Anchor Canyon rocks, when compared to known igneous rock series, are seen to best follow that of the calc-alkaline trend.

The pluton was emplaced at a minimum depth of between 3,000 and 4,000 feet by a passive injection of magma along a

major fault zone. The magma at the time of emplacement had the composition of type I, augite-quartz monzonite, and a temperature in the vicinity of 790°C.

Initial crystallization was intratelluric and began with the precipitation of plagioclase, augite, and accessory minerals followed later by hornblende and biotite. The ascent into the upper crust was characterized by a drop in pressure and concentration of volatiles causing partial resorption of plagioclase and hornblende. Solidification of the already crystal-rich magma began marginally and progressed inward with rapid growth of alkali feldspar and quartz. The final stages of crystallization had many complexities due to the action of residual liquids. Trapped aqueous solutions account for the occurrence of small amounts of aplitic and pegmatitic material.

CONTENTS

ILLUSTRATIONS

Frontispiece: The Magdalena Mountains looking south southeast with Anchor Canyon in the foreground.

FIGURES

INTRODUCTION

Location and Distribution

The Anchor Canyon stock is situated at the north end of the Magdalena Mountains seventeen miles west-northwest of Socorro in the Magdalena Quadrangle, Socorro County, New Mexico (fig. 1), between the coordinates 107° 11' and 107° 12' 30" West Longitude, 34° 06' 30" and 34° 08' 45" North Latitude.

The pluton outcrops in a 2½ square mile area and forms the east side and entire ridge on the west side of Anchor Canyon (fig. 2). Its northern border is covered by alluvium, but the presence of contact metamorphic minerals on prospect dumps in the upper part of the Sandia Formation southeast of Granite Mountain suggests that the intrusive may extend nearly that far north.

A small stock of granite, identical in appearance to the Anchor Canyon stock, outcrops on the west side of Granite Mountain, but is not included in this study. Other similar rocks include a granite dike intrusive into typical monzonite on the north end of Stendel Ridge and granite just north and northeast of the Oak Spring location as a local differentiate of monzonite (Loughlin and Koschmann, 1942, p. 39).

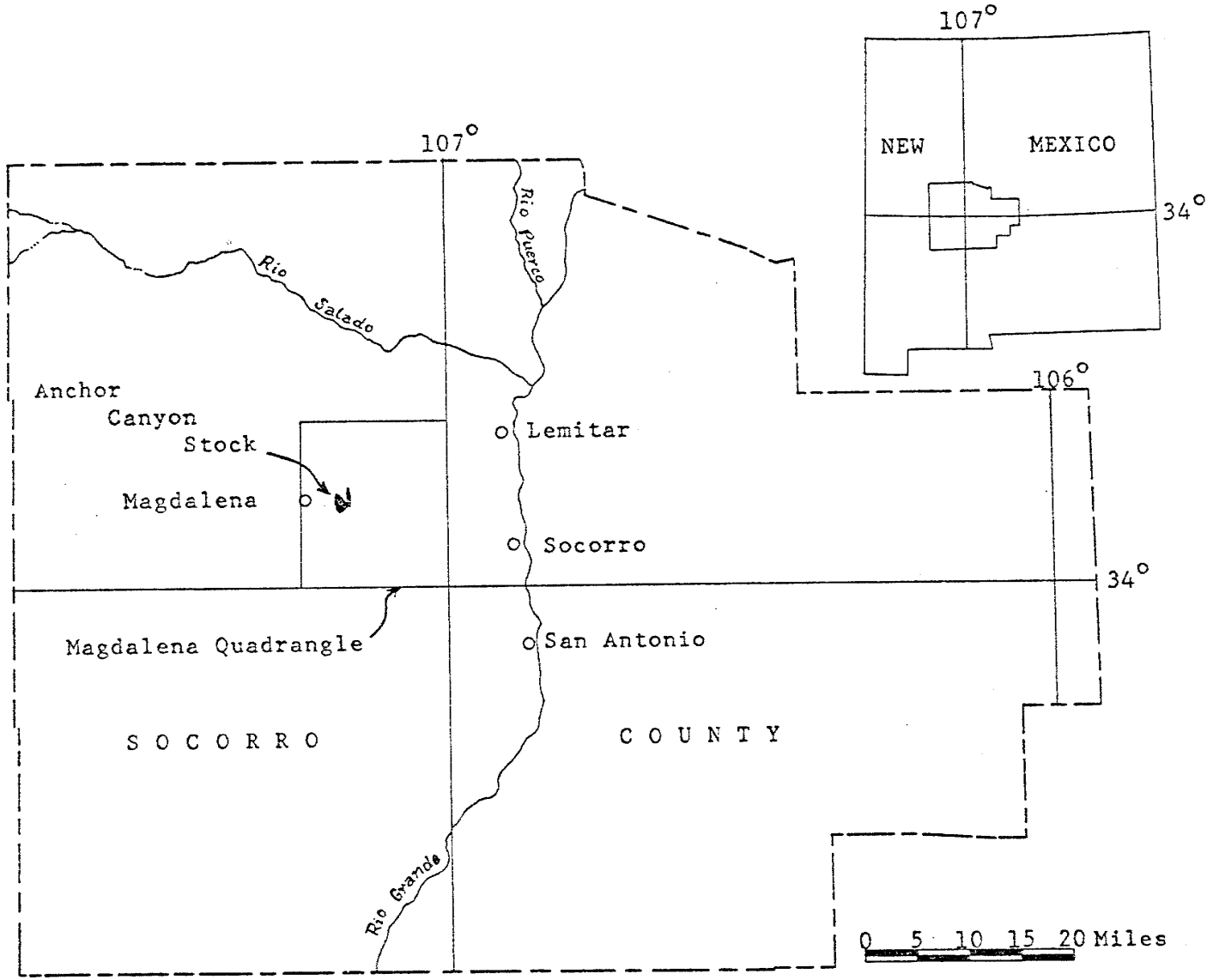

Figure 1.--Index map showing location of the Anchor Canyon stock.

Figure 2

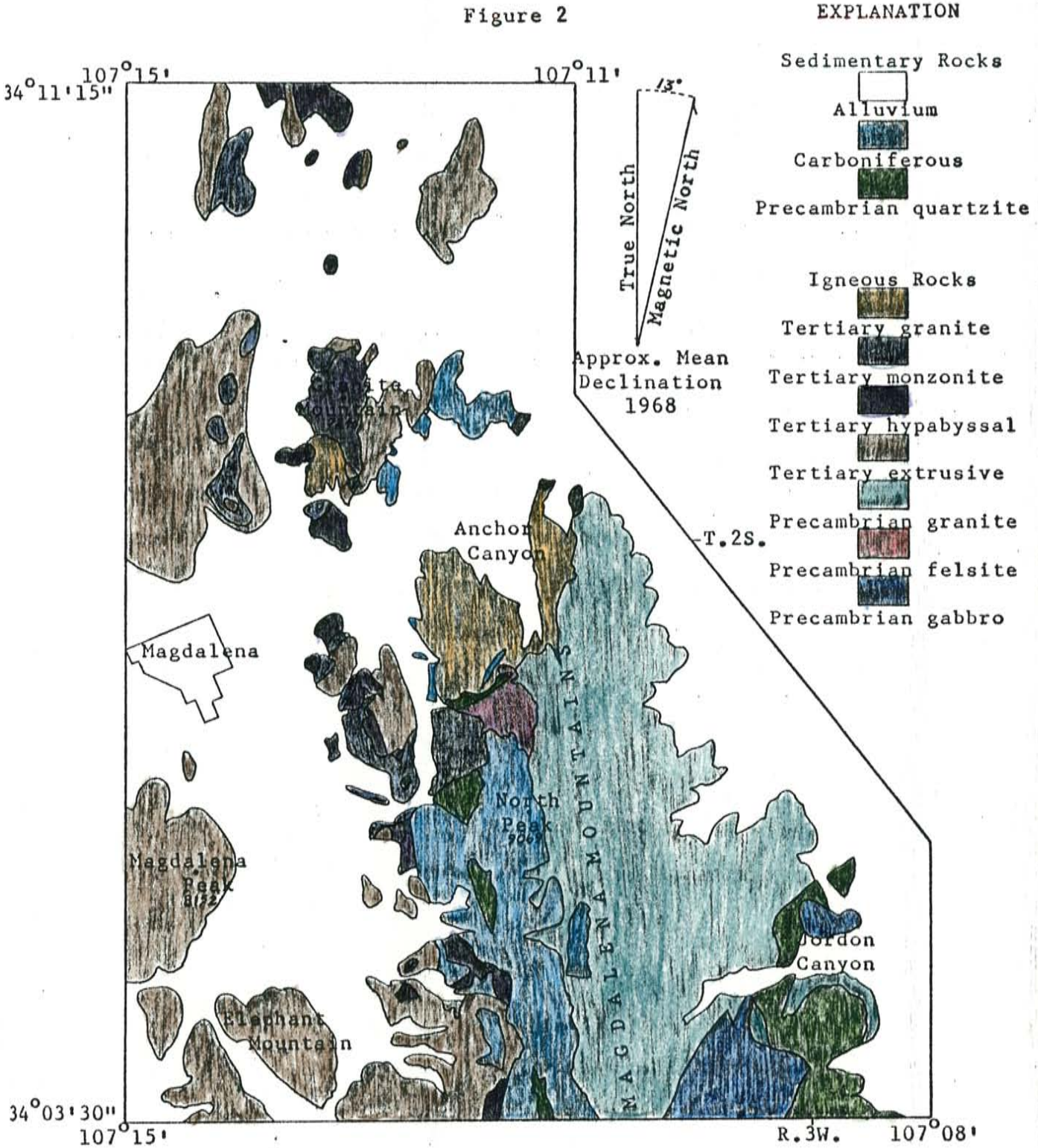

GEOLOGIC MAP OF THE MAGDALENA AREA
SOCORRO COUNTY, NEW MEXICO

Scale 1:75100

1 ½ 0 1 2 3 Miles

Reconnaissance mapping to the north and west of Anchor Canyon by Winchester (1920) and Johnson (1955) failed to show further outcrops of granitic rocks other than those noted above.

Previous Work

Rocks of the Anchor Canyon stock were first described by Gordon (1910, p.247-248). He cites three rock types: a quartz monzonite porphyry, a quartz monzonite, and a granite porphyry as occurring in the area of Anchor Canyon. Since his work dealt mainly with ore deposition, his descriptions are brief and general. His Plate XVII (p.252) is a geologic sketch map of the Magdalena Mining District on a scale of 1 : 21,120. The mapping is incomplete with most of the rock types undelineated.

Lasky (1932, p.22) mentions, in passing, the presence of small stocks of monzonite and monzonite porphyry having quartzose and granitic phases in the Magdalena district. He sets their age at early Tertiary.

The most detailed study of the Anchor Canyon stock was made by Loughlin and Loschmann (1942, p.39-47) as part of a study dealing with the ore deposits in the Magdalena Mining District. Their Plate 2 is a geologic map of the Magdalena district drawn to a scale of 1 : 12,000. On this map, the stock is well defined and is mapped as Tertiary (?) granite. Their rock descriptions have been made largely from samples

taken near the Hardscrabble mine and along the western ridge of Anchor Canyon from which they describe a porphyritic and a non-porphyritic facies.

Recent K/Ar dates for the Anchor Canyon and Nitt stocks as well as for volcanics in the area are reported in a brief chronologic summary by Kottlowski, Weber and Willard (1969). A more complete report may be found in Weber (1971).

Methods of Investigation

Field Work

Field work consisted of a systematic sampling of the pluton, investigation of the contact relationships and modification of a portion of the geologic map made by Loughlin and Koschmann (1942) (fig. 3-4) who used the Magdalena District topographic map on a scale of 1 : 12,000 (fig. 5) as a base. A geologic map of the Magdalena area (fig. 2) was made by combining the work of Loughlin and Koschmann (1942) and Johnson (1955) with original work by the author on the northeastern slopes of the Magdalena Mountains, and plotting this information on the Magdalena Quadrangle (fig. 6), which is on a scale of 1 : 62,500.

Sampling of the Anchor Canyon stock followed a rectangular grid pattern spaced 750 feet apart; this pattern was rigidly adhered to during the collection of samples. Seventy-two specimens were collected in all. Some of the advantages of such a sampling are discussed by Whitten (1961) and Exley (1963). The advantages include: an unbiased sampling, consideration of the third dimension, and simplification of the statistical aspects of the data.

Laboratory Work

Laboratory work included modal analyses of each specimen, petrographic and mineralogic investigation of each rock type, and chemical analyses of selected samples. Modal analyses

Figure 3

GEOLOGIC MAP OF THE ANCHOR CANYON STOCK

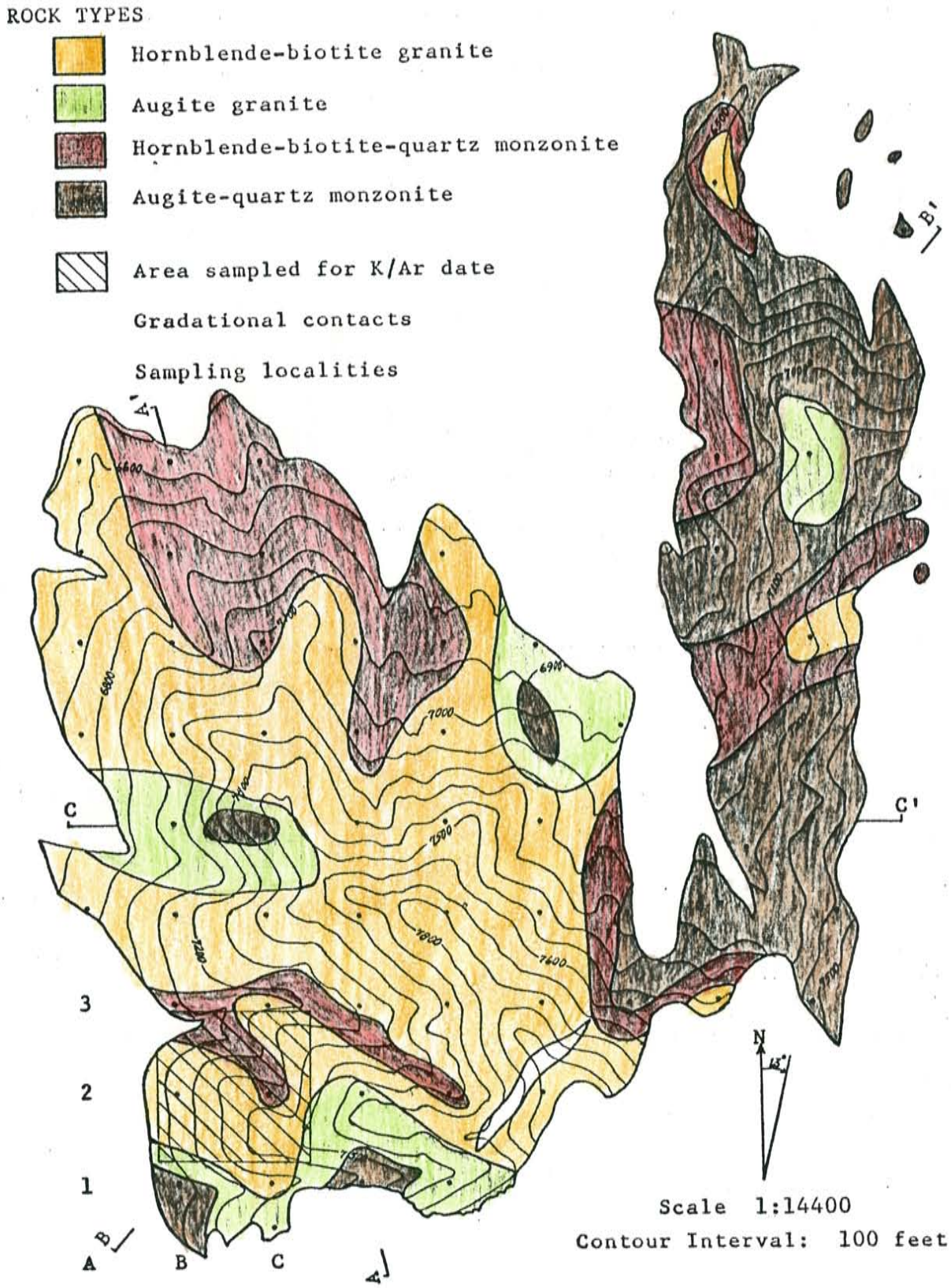

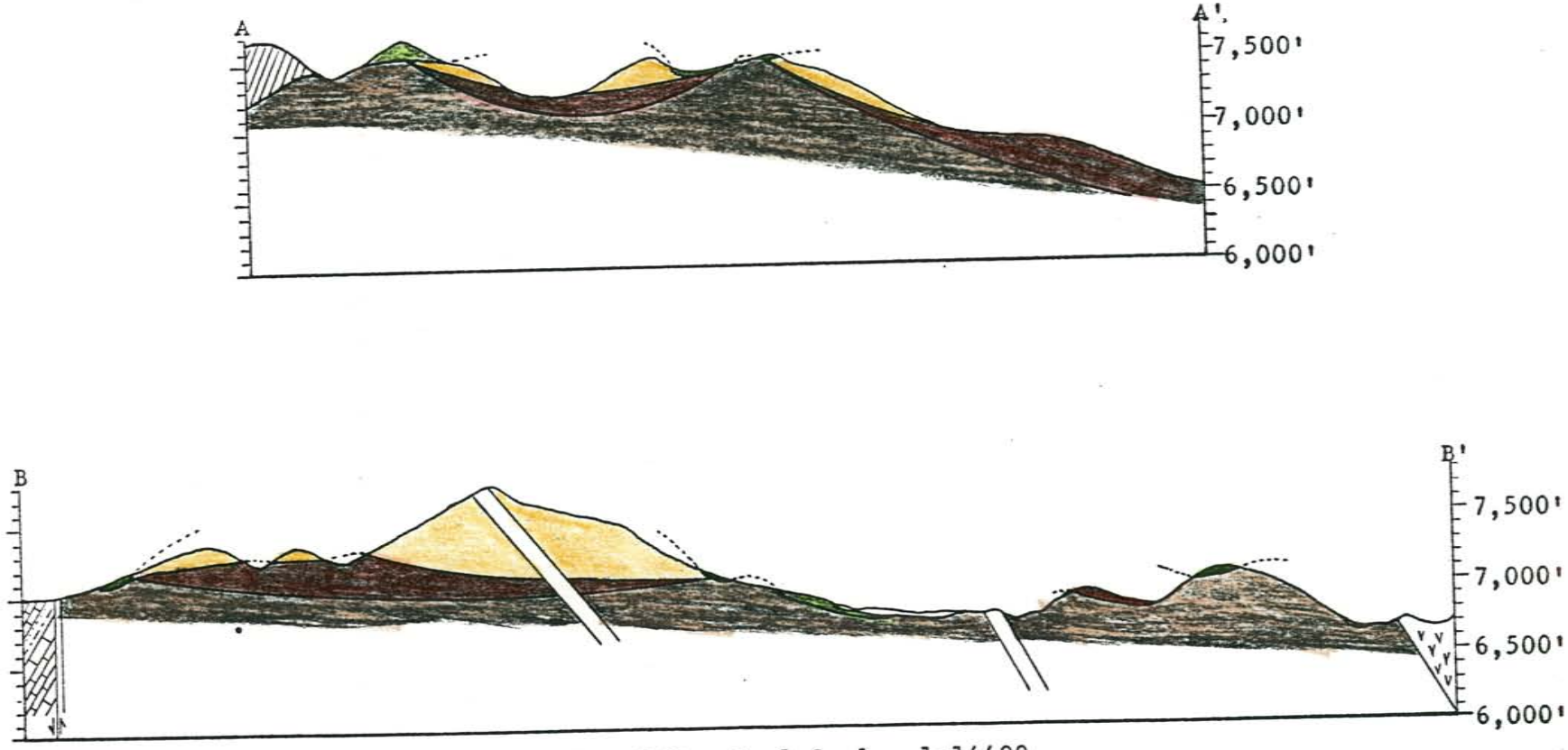

Horizontal and Vertical Scale 1:14400

SECTIONS ALONG LINES A-A' AND B-B' OF FIGURE 3
(Section C-C' included in Figure 23)

Figure 4

were made on a J. Swift and Son electric point-counter. One thousand points were counted per thin section, with points 0.3 mm apart in traverses spaced at 1.0 mm. A chart for judging the reliability of point counting has been developed by Van der Plas and Tobi (1965) and indicates that the error in the present analyses is between zero and three percent depending upon the volume percent of the mineral. Further information on the limitations and errors in point counting are reported by Chayes (1956), Hasofer (1963), and Solomon (1963). Chayes emphasizes the importance of the interrelationship between grain-size, area covered, and grid spacing, in the estimation of volume percent. He also warns of the error involved in making modal analyses of inequigranular rocks. Solomon recognizes three principle sources of error: (1) operator error: mis-identification, (2) counting error: introduced during estimation of areal fractions, (3) sampling error: introduced in estimating the composition of a volume from one or more areal analyses.

Petrographic analyses were made with a Leitz student model petrographic microscope and a Zeiss-Winkel four-axis universal stage, mounted on a Zeiss research microscope. Mineral identification and composition determinations were made with the aid of diagrams from Emmons (1943), Kerr (1959), and Tröger (1959). A polished thin section was prepared for an electron probe analysis of biotite to help in the identification of rutile.

Ten samples were analyzed for eight major elements (Si, Al, Ti, Fe, K, Ca, Na, and Mg) and six trace elements (Rb, Sr, Ba, Cu, Zn, Ni) by non-destructive X-ray fluorescence. Analytical methods are those used by Condie (1967). The estimated total error is less than five percent.

Geography

Topography and Relief

The Magdalena Mountains have a north-south trend and in the mapped area descend in elevation northward. At the northern end, long, sloping canyons extend eastward from the main range. At the mouths of these canyons, large alluvial fans have formed marking the upper slopes of the pediment. The intervening ridges are rounded to jagged in outline and are narrow with steep, rugged slopes. These slopes are usually veneered with a thin cover of talus giving them a smooth look. The west side of the range is characterized by shorter canyons and a more even appearance on the upper slopes, diminishing to an irregular appearance on the lower slopes. The drainage pattern is dendritic, but appears somewhat rectangular.

Anchor Canyon is a north facing canyon and has 1,700 feet of relief. The steepest slopes occur at the uppermost end of the canyon.

Outcrops

Exposures are plentiful on the upper slopes, with the best found along ridges and in canyons (fig. 7a). Outcrops on the lower slopes are less easy to distinguish from large boulders, partly buried in colluvium.

Acknowledgments

The writer is indebted to Professors A. J. Budding, C. E. Chapin and K. C. Condie, Department of Geosciences, New Mexico Institute of Mining and Technology, for helpful suggestions and critical reviews of the paper. Thanks are also due Michael Murray for computer programming assistance, Corale Brierly for an electron-microprobe analysis, and the Department of Metallurgy, New Mexico Institute of Mining and Technology and the New Mexico Bureau of Mines and Mineral Resources for the use of their X-ray equipment.

Financial support for the making of thin sections came from the New Mexico Geological Society.

GEOLOGIC SETTING

General Statement

The Anchor Canyon stock is the largest of several stock-like bodies exposed at the north end of the Magdalena Range. Rocks exposed in the Magdalena Mountains are of Precambrian, Paleozoic, and Tertiary Age.

The geologic history of the Magdalena Mining District was worked out by Loughlin and Koschmann (1942). The Precambrian basement complex consists of metamorphosed quartzose to argillaceous sediments which were folded and successively intruded by a gabbro sill, a felsite body, a granite pluton, and diabase dikes. Paleozoic limestones, sandstones and shales were deposited unconformably upon the eroded Precambrian rocks. The Laramide Orogeny elevated and tilted the entire block westward forming the Magdalena Mountains as an anticlinal structure. Minor folds parallel to the major north-northeast anticlinal axis and east-west trending faults also developed. A period of Tertiary volcanism (37-30 m.y.) was followed by plutonism (28 m.y.) including the intrusion of the Anchor Canyon stock. Subsequent faulting uplifted and tilted the range further westward. Final igneous activity was characterized by the intrusion of dikes and sills of various composition.

Host Rocks of the Anchor Canyon Stock

Quartzite

Quartzite (argillite by Loughlin and Koschmann, 1942) was derived from an argillaceous to quartzose sandstone and is most abundant just north of Water Canyon (see fig. 2). Smaller bodies lie along the western side of the Magdalena Mountains. Two small wedges are in contact with the Anchor Canyon stock, the larger of which occurs along the southern periphery between the pluton and Precambrian felsite and strikes northeast with an average dip of 70° southeast. The smaller wedge is located on the northeast side of Anchor Canyon and is in fault contact with Tertiary granite. Here it strikes north-northeast and dips 80° southeast.

Tertiary banded rhyolite, so labeled by Loughlin and Koschmann, is more likely a highly metamorphosed facies of Precambrian quartzite which had undergone thermal metamorphism during the emplacement of the pluton.

Felsite

Felsite is found principally in a triangular area immediately to the south of the Anchor Canyon stock. It is dark purplish to black on fresh surfaces, dense to extremely fine grained and contains small phenocrysts. It lies in contact with the stock for about 300 yards across the top of a ridge along the southern margin.

Granite

The largest single body of rock in the area is a granitic pluton of Precambrian age which borders the Anchor Canyon stock on its eastern side. The granite is pink in color and, in this area, finer grained and poorer in biotite than it is further to the south.

Paleozoic Rocks

Paleozoic rocks are of Mississippian, Pennsylvanian, and Permian Age with Pennsylvanian rocks predominating. The Pennsylvanian rocks consist of interbedded limestones, sandstones, and shales which flank the lower western slopes of the Anchor Canyon stock. The beds strike due north and have a dip of approximately 65° west. Paleozoic rocks are more extensive to the south where they rest upon Precambrian rocks; their dip is somewhat less, averaging between 45° and 50° west. A large inclusion of Mississippian limestone, striking northeast and dipping 65° to the southeast, lies near the southeast border. The limestone mass is about 1,400 feet long, up to 150 feet wide, and extends northward beyond the crest of the range.

Nitt Stock

The Nitt stock is the largest of several monzonitic stocks in the district. It lies south-southwest of the Anchor Canyon stock. Isolated bodies of monzonite in this vicinity and on Stendel Ridge are also part of the Nitt stock since

monzonite underlies the alluvium separating them. Within the Nitt stock, just north and northeast of Oak Spring (fig. 2), granite occurs as a local differentiate. Typical monzonite is medium-grained but it is fine-grained and darker in color in marginal facies. Of particular note is the northerly alinement of monzonitic stocks in the Magdalena district.

Age

Potassium-argon dates have been reported for the Anchor Canyon and adjacent Nitt stock by Weber and Bassett (1963) and are given in Table I. The sample of monzonite was taken from an outcrop southwest of the Hardscrabble mine 2½ miles southeast of Magdalena, S.E. ¼ Sec. 25, T.2S., R.4W. The granite sample was taken from a roadcut 2½ miles east of Magdalena, N.E. ¼ N.E.¼ Sec. 25, T.2S., R.4W. The samples were dated by Bassett at the Brookhaven National Laboratory. The monzonite gave an age of 28.0 m.y., and the granite an age of 28.3 m.y.

The age relationship as observed in an outcrop at the southwest corner of the Anchor Canyon stock shows monzonite intruded by granite (fig. 7b). Loughlin and Koschmann (1942) have not indicated this contact on their map; however, they deduced the same relation by noting that a granite dike intruded typical monzonite on the north end of Stendel Ridge and by contact relations on Granite Mountain.

The ages reported would indicate that the monzonite is younger than the granite, however, both dates fall within the range of the experimental error of approximately 5 percent. In any case, the two stocks are closely associated in time and space.

Figure 7a
Outcrop of Tertiary granite in upper part of Anchor Canyon

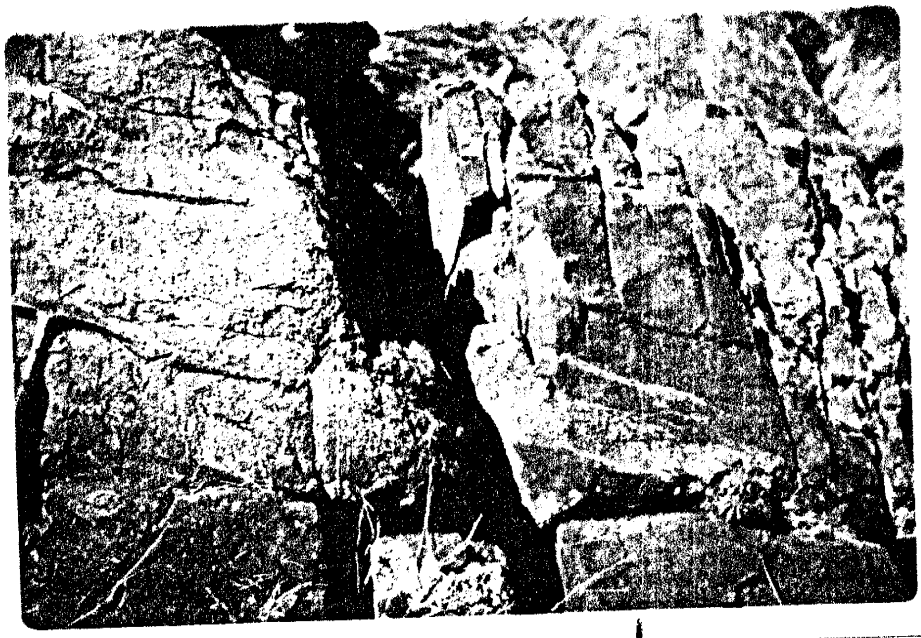

Figure 7b
Tertiary monzonite (gray) intruded by Tertiary granite (light gray, speckled)

ROCK TYPES

The Anchor Canyon stock can be divided into four rock types based on their modal percentages of perthitic alkali feldspar, plagioclase, ferro-magnesian minerals, and texture (Table II). Modal and chemical analyses are listed in Tables III and IV respectively. The four rock types present are: augite-quartz monzonite, hornblende-biotite-quartz monzonite, augite granite, and hornblende-biotite granite. A plot of the Rb/Sr ratios as with one of the alkali-lime index (Peacock, 1931) (fig. 8) shows rocks to be mildly alkaline and thus they could more properly be named alkali-granites and alkali-quartz monzonites. Figure 9 shows the rock samples of Table III plotted in terms of modal quartz, alkali feldspar, and plagioclase feldspar recalculated to 100 percent. The boundary lines for the classification by Travis (1955) have been superimposed on the diagram. The 40 percent quartz boundary line is that of Chayes (1957). The gradational character of the rocks is evident from this diagram.

In general, the rocks, are porphyritic to sub-porphyritic, medium- to fine-grained, and have granophyric to hypidiomorphic-granular textures (fig. 10a, 10b). The finer-grained phases could be more aptly termed granophyre. One of the rocks' more striking features is a cumulophyric texture represented by aggregates of white plagioclase, green

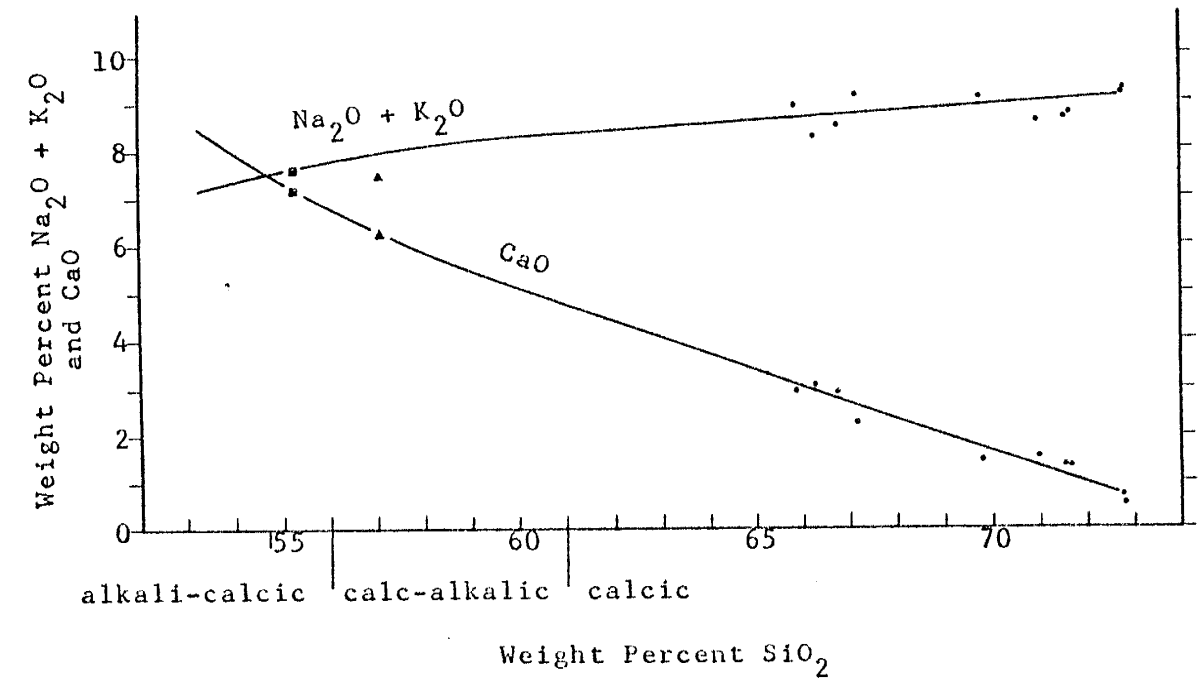

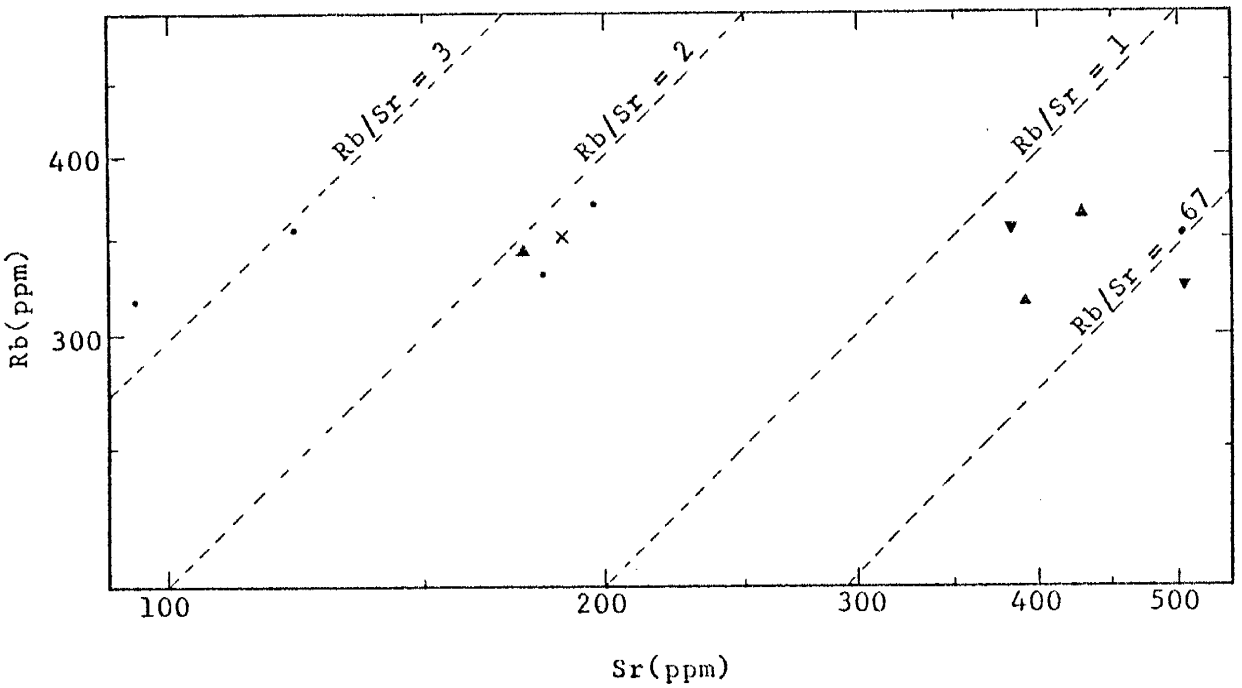

Figure 8. (above)Alkali-lime plot after Peacock(1931); dots-rocks from the Anchor Canyon stock, triangles-monzonite from the Nitt stock(Loughlin and Koschmann,1942,p.39), squares-average analysis of monzonite(Daly,1914,p.23). (below)Log-log plot of rubidium versus strontium; deltas: augite-quartz monzonite, triangles: hornblende-biotite-quartz monzonite, cross: augite granite, dots: hornblende-biotite granite.

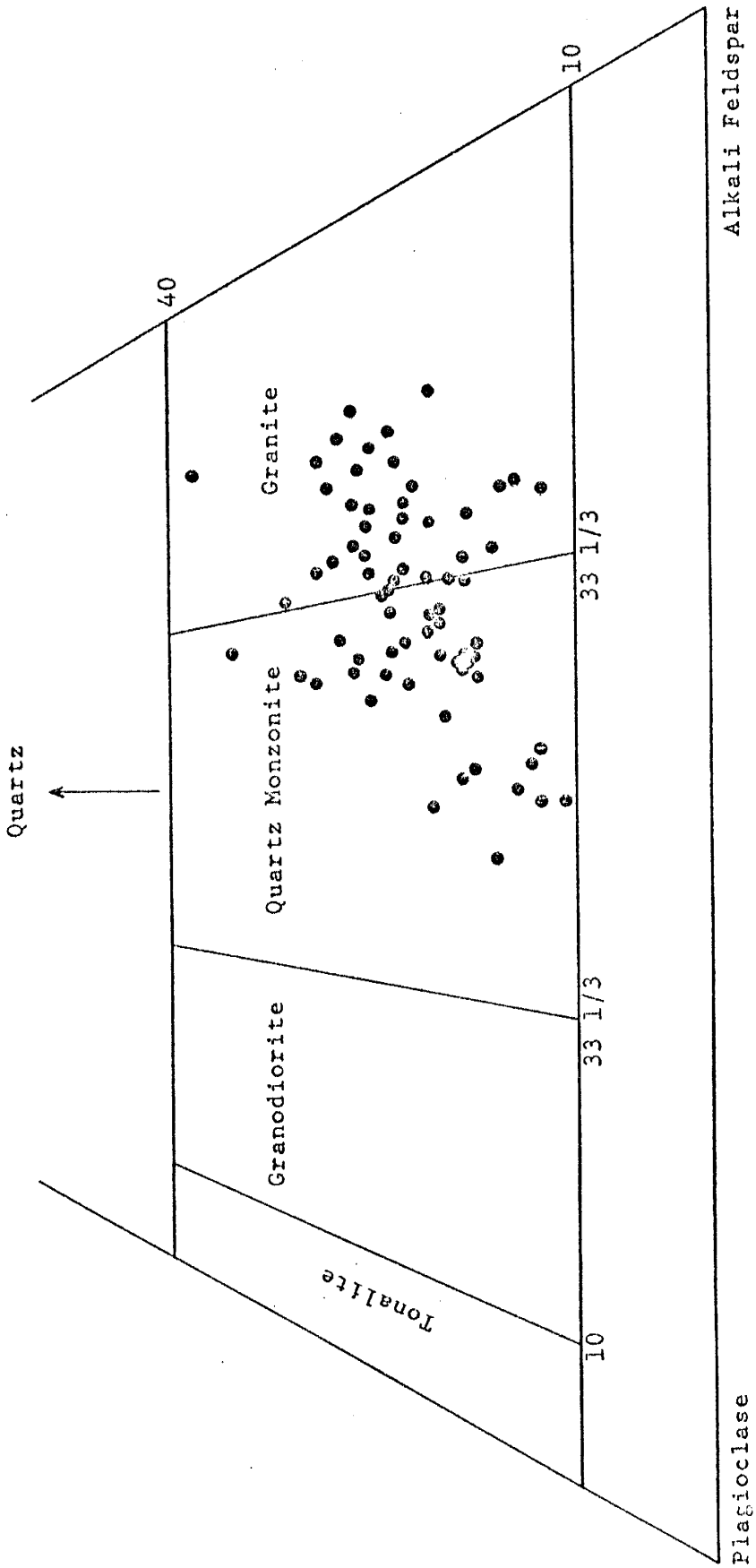

Figure 9. Classification scheme used for granites and quartz monzonites from the Anchor Canyon stock. Modal quartz, plagioclase, and alkali feldspar recalculated to 100 percent.

Figure 10a
Photomicrograph showing the texture of Tertiary granite. Gray - alkali feldspar, clear - quartz, light-gray - plagioclase (plane polarized light) (specimen E1)

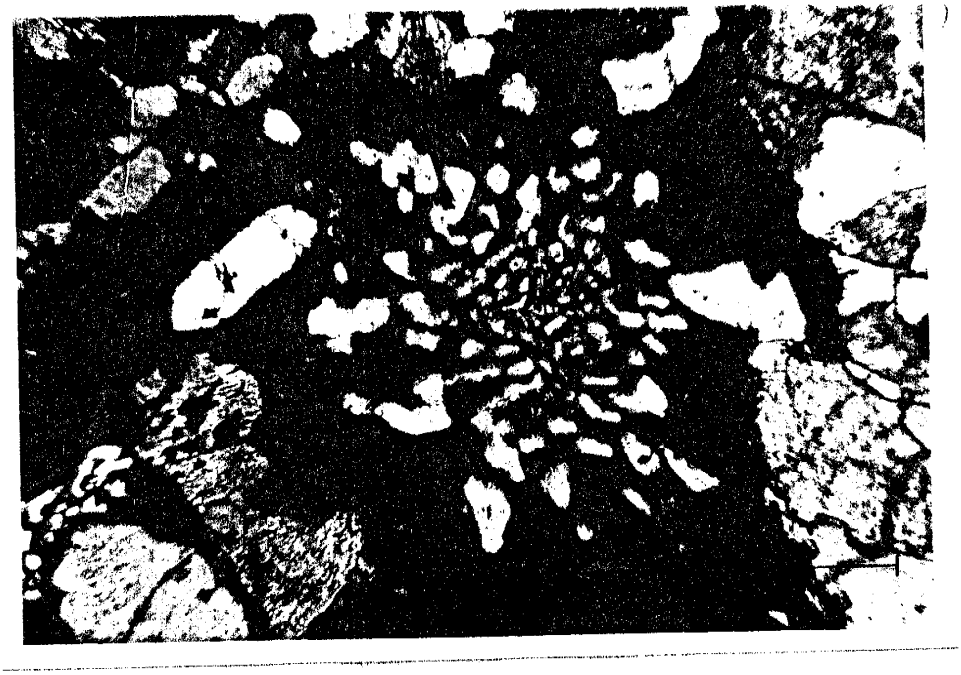

Figure 10b
Graphic intergrowth of quartz and alkali feldspar Clear - quartz, gray - alkali feldspar (plane polarized light) (Specimen B2)

hornblende, biotite and occasionally augite. Phenocrysts are of pink to gray alkali feldspar and white, sometimes opalescent, plagioclase. The rock is leucocratic; the color varies from light- to dark-pinkish gray with increasing grain size and weathers to buff. Another distinctive feature in hand specimens from the pluton is an apparent lack of quartz, but after close examination this mineral is found to be fairly abundant. Since the rocks are gradational with each other, the contacts shown in Figure 3 are somewhat arbitrarily drawn.

Outcrops are usually subdued and the rocks exhibit spheroidal weathering. Where the rocks are of finer grain size, the outcrops are more angular in outline.

Type I: Augite-quartz Monzonite

Type I, augite-quartz monzonite, is present in a zone along the eastern border which extends westward into Anchor Canyon where it is covered by alluvium. It also occurs in a deep ravine along the southern border and in two isolated locations on either side of the western ridge. It has a marked cumulophyric and porphyritic texture. Phenocrysts of plagioclase comprise between 15 and 25 percent of the rock and are embedded in a medium-grained groundmass, which changes to fine-grained eastward. The matrix ranges in grain size from 0.7 mm to 3.0 mm with phenocrysts rarely exceeding 1 cm in size. The color is pinkish gray, darkening with increasing mafics and grain size at the uppermost end of Anchor Canyon. Yellow specks of sphene are quite common in this rock type.

Type II: Hornblende-biotite-quartz Monzonite

Type II outcrops along the lower slopes on the east and west side of Anchor Canyon and within the side canyon that leads up to the Hardscrabble mine. It is similar to Type I, but lacks augite and has a less pronounced cumulophyric texture. The rock contains between 5 and 10 percent phenocrysts of plagioclase and alkali feldspar, usually not larger than 5.0 mm embedded in a matrix ranging in grain size from 0.5 mm to 1.5 mm in length. Type II hornblende-biotite-quartz monzonite grades into Type IV, hornblende-biotite granite at higher elevations.

Type III: Augite Granite

Type III is the least abundant and occurs in four localities: one on either side of the western ridge, one midway up the eastern side of Anchor Canyon, and one along the southern boundary of the stock. It varies in texture from medium-grained porphyritic on the eastern half to a fine-grained subporphyritic rock on the western half of the pluton. Type III grades into Type IV in the central portion of the pluton.

Type IV: Hornblende-biotite Granite

Type IV mantles the ridge and spurs west of Anchor Canyon on down to the alluvium toward the northwest. It also occurs in two small, isolated areas on the eastern side of Anchor Canyon. The texture is predominantly granophyric

having a grain size between 0.2 mm and 1.0 mm. Phenocrysts make up from 1 to 10 percent of the rock with plagioclase phenocrysts decreasing westward relative to phenocrysts of alkali feldspar. Miarolitic cavities lined with quartz, epidote and black tourmaline are a common occurrence. Also peculiar to this rock is the formation of rutile needles along biotite cleavage planes. Mafics are much decreased in volume percent with the exception of two samples taken near the limestone inclusion. Zeolites are of rare occurrence.

Aplitic and Pegmatitic Phases

A finer-grained, lighter colored variant is frequently observed in the hornblende-biotite granite and to a lesser extent in the hornblende-biotite-quartz monzonite. They are generally dike- or sheet-like in appearance and vary in size from a few inches to a foot in thickness. Boundaries are usually abrupt, but at one location near the southern end of the pluton, the finer-grained facies was distinctly gradational into the hornblende-biotite-quartz monzonite. The rock differs from its host rock in that it lacks conspicuous dark minerals being composed almost entirely of feldspar and quartz and having an allotriomorphic-granular texture. All mineral grains are approximately equal in size averaging 0.1 mm in diameter.

A more infrequent occurrence is that of pegmatitic material which forms small elongated pods seen mainly on the western side of Anchor Canyon. They consist largely of pink

alkali feldspar graphically intergrown with quartz. Other occurrences reported by Loughlin and Koschmann (1942, p.41) include along the contact east of Hardscrabble mine and on the crest of the ridge east of Anchor Canyon where a short veinlet containing black tourmaline, feldspar, and quartz cuts Precambrian granite and is thought to represent material from the Anchor Canyon stock.

Mineral Descriptions

The major mineral constituents in rocks of the Anchor Canyon stock are plagioclase, orthoclase microperthite, quartz, biotite, hornblende, and augite. Accessory minerals are magnetite, apatite, sphene, zircon, allanite, and more rarely schorlite and fluorite. Secondary minerals include epidote, chlorite, sericite, rutile, calcite, hematite, pyrite, leucoxene, and less commonly siderite and muscovite. Optical properties of the major minerals are listed in Table V.

Plagioclase occurs in two habits: anhedral phenocrysts averaging 5.0 mm in length with polysynthetic albite twinning, combined Carlsbad-albite twinning, or albite-pericline twinning; and subhedral grains averaging 1.0 mm and exhibiting albite twinning only. Phenocrysts generally have oscillatory-zoned cores of andesine-labradorite and rims of oligoclase with normal zoning from An_{30} to An_{24}. Core compositions range between An_{35} and An_{56} and are almost as variable within an individual thin section as in the entire pluton. In phenocrysts, the part with oscillatory zoning predominates over the normal zoned portion implying a low rim/core ratio

(Vance, 1962). The boundary between core and rim is seen by a sharp drop in An content and is usually outlined by incipient sericitization. This discontinuity, although, in some cases euhedral, may be further marked by irregular embayments and patches of rim material within the cores. Occasionally rims truncate oscillatory zoning.

Inclusions in phenocryst cores are few but when seen include magnetite, zircon, and biotite. Close examination of one core revealed a minute rod-shaped mineral regularly spaced and appearing to parallel plagioclase cleavage planes. Plagioclase in the groundmass is typically free of inclusions and may show slight normal zoning. The composition of matrix plagioclase and the outermost zone of phenocryst rims are the same. Plagioclase phenocrysts commonly show signs of deformation such as off-set twinning and irregular extinction patterns especially near intrusive margins.

Sericitization is absent to scant in most grains and is more common in the granitic varieties. Alteration occurs marginally and along fractures. A pale-brown mineral, with low index of refraction and moderate birefringence, locally accompanies sericite and was also noted by Loughlin and Koschmann (1942, p.40) who place it in the montmorillonite-beidellite group. According to Carrigy and Mellon (1964), it is most likely montmorillonite.

Alkali feldspar is predominantly orthoclase microperthite. Phenocrysts up to 1 cm in length are euhedral and strongly poikilitic containing inclusions of plagioclase,

biotite, zircon, allanite, apatite, magnetite, hornblende, pyroxene, and quartz. Anhedral to subhedral grains interstitial to plagioclase and sometimes quartz range in size from 0.5 mm to 1.5 mm. Micrographic intergrowths with quartz occurs just within the boundary of grains and interstitially. Quadrille structure is almost entirely absent. Myrmekite is also present, but not common. "Antirapakivi" mantling of alkali feldspar on plagiocalse (fig. 11a) and more rarely as an outer zone on less perthitic alkali feldspar is an occasional phenomenon. Rapakivi mantling was also observed (fig. 11b).

The axial angle, $2V_x$, using the extinction method, ranges from about 59^o to 72^o. This variation in optic axial angle is present from grain to grain in the same thin section and is ascribed by Tuttle and Bowen (1958, p.105-107) to be a result of partial inversion from a higher temperature form. X-ray diffraction studies were made on two hand-picked feldspars from samples B8 and H10 using an internal standard of 5 percent silicon. Table II of Wright and Stewart (1968, p.76-77) shows conclusively that alkali feldspar is orthoclase, and by comparison with Figure 3 of Wright (1968, p.92) it may be termed anomalous. The significant 2θ values for CuK_a radiation are listed in Table VI. Examination of alkali feldspars from samples E1 and E8 by the powder method substantiated the previous results. The masking of orthoclase by minute dustlike inclusions is universal and complete in most grains. In some phenocrysts, masking is restricted to the

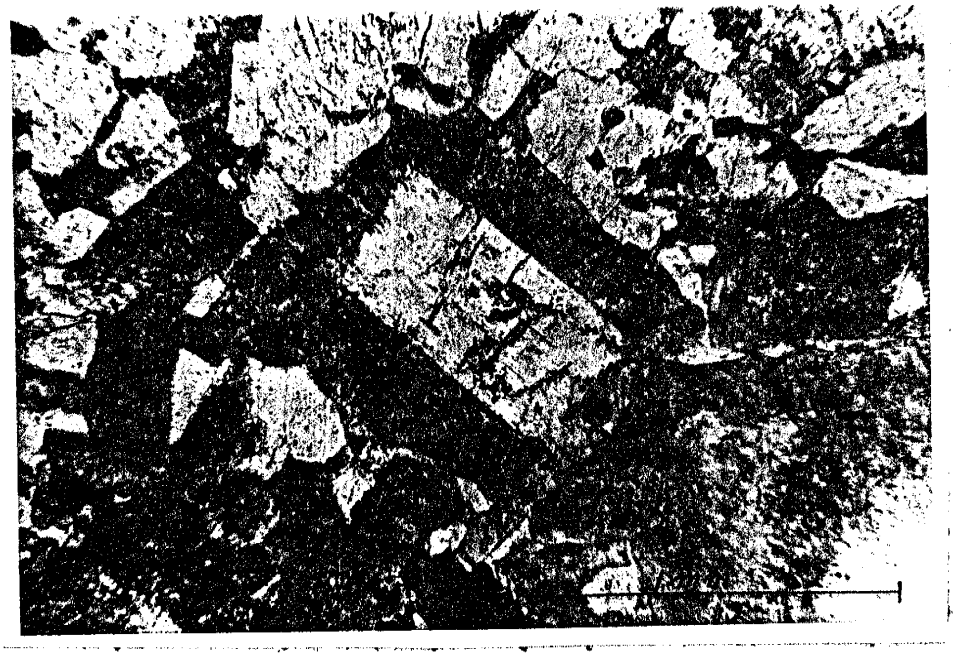

Figure 11a
Mantling of alkali feldspar on plagioclase
Center photo - plagioclase, gray - alkali feldspar (plane polarized light) Specimen E5

Figure 11b
Alkali feldspar mantled by plagioclase
Gray (center photo) - alakali feldspar, clear - plagioclase (X - nicols) (A9)

margins leaving the centers clear. Sericite is probably the most abundant inclusion with hematite an obvious associate attested to by the pink color of the feldspar. The effects of strain and crushing is evident in samples taken near the edge of the pluton.

Quartz forms irregular grains generally less than 1.0 mm, but occasionally as much as 2.0 mm in length. The most common forms are groundmass granules forming interlocking aggregates with other quartz grains and orthoclase and extensive irregular interstitial masses. Now and then, small euhedral grains occur as inclusions in orthoclase. Quartz is also, in part, graphically intergrown with orthoclase and less commonly with plagioclase as a replacement of orthoclase. As with the feldspars, quartz exhibits undulatory extinction near the fringes of the pluton.

Pale yellow to dark red-brown biotite is the most abundant mafic mineral. Laths, more or less bent throughout, average 1.5 mm in length, but will attain sizes of up to 3.0 mm. Tabular sections commonly yield euhedral terminations. Inclusions present are magnetite, apatite, plagioclase, zircon and allanite. Magnetite granules occasionally exhibit a circular pattern within biotite marking what was apparently an old crystal boundary (fig. 12). Pleochroic haloes around zircon are faint to absent. Peculiar to biotite of the hornblende-biotite granite is the occurrence of minute needles of rutile in regular orientation paralleling the (110), (010), and $(1\bar{1}0)$ crystallographic planes and lying in the (001) plane.

Figure 12
Magnetite marking a former crystal boundary in biotite
Gray - biotite, black - magnetite (plane polarized light)
(Specimen I7)

Needles average one micron in width and are never present near grain margins nor found elsewhere in the rock (fig. 13a,b). Smedes (1966, p.73) reports a similar occurrence. The dark red-brown color of biotite attests to either its high titanium content alone or to a high TiO_2/FeO ratio (Engel and Engel, 1960).

Alteration of some biotite grains to chlorite is present on grain edges and cleavages. In four thin sections, conversion to chlorite is complete. Locally, biotite alters to a dark brownish green and, to a much less extent, a yellow-green biotite. Muscovite on rare occasions replaces biotite along zones parallel to the (001) cleavage.

Actinolitic hornblende is light bluish green to blue green in color and may locally exceed biotite in abundance. Three habits occur: subhedral to anhedral grains in parallel position on augite cores (fig. 14a,b), discrete euhedral to subhedral grains and aggregates commonly twinned (fig. 15a), and interstitial grains and columnar aggregates filling cavities (fig. 15b). Uralitic hornblende (Deer, Howie and Zussman, v.2, p.260) has a darker shade of pleochroic colors and is ordinarily largest in size with individual grains up to 3.0 mm in length. Its occurrence is necessarily restricted to the augite-bearing rock types. The second habit is widespread typically as prismatic crystals having a size range from 1.0 mm to 1.5 mm in length. It is least abundant in the hornblende-biotite granite where it has a distinct shredded appearance. Magnetite, plagioclase, apatite, and zircon are

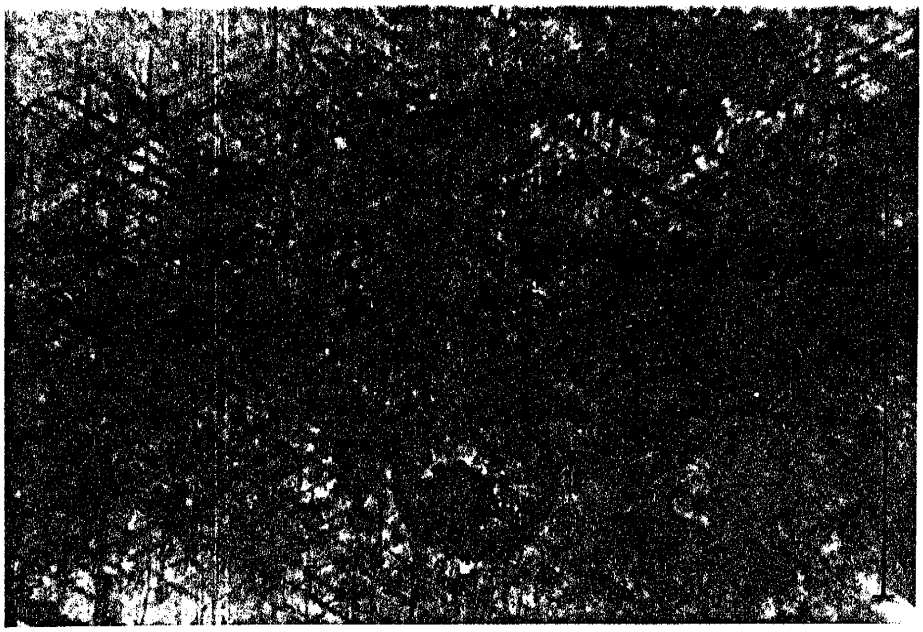

Figure 13a
Photomicrograph of rutile needles in biotite (plane polarized light) (Specimen A7)

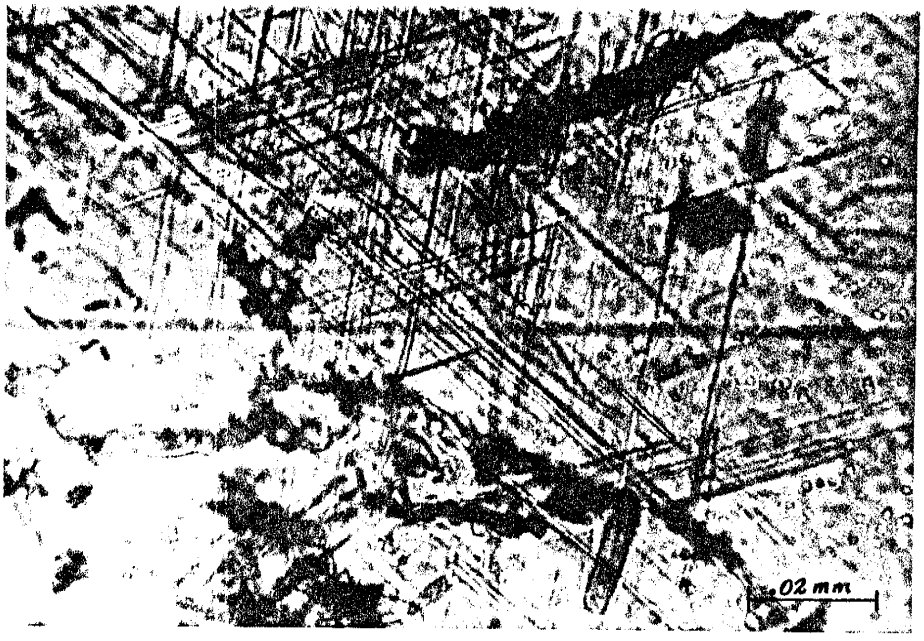

Figure 13b
Same as above (higher power)

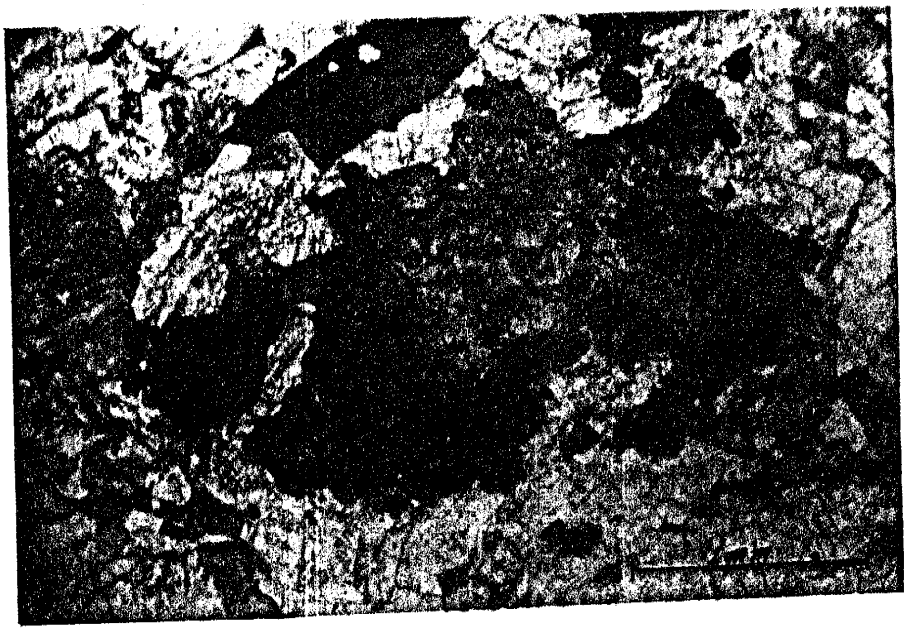

Figure 14a
Photomicrograph of hornblende after augite (plane polarized light) Dark - hornblende, clear (center) augite (Specimen B1)

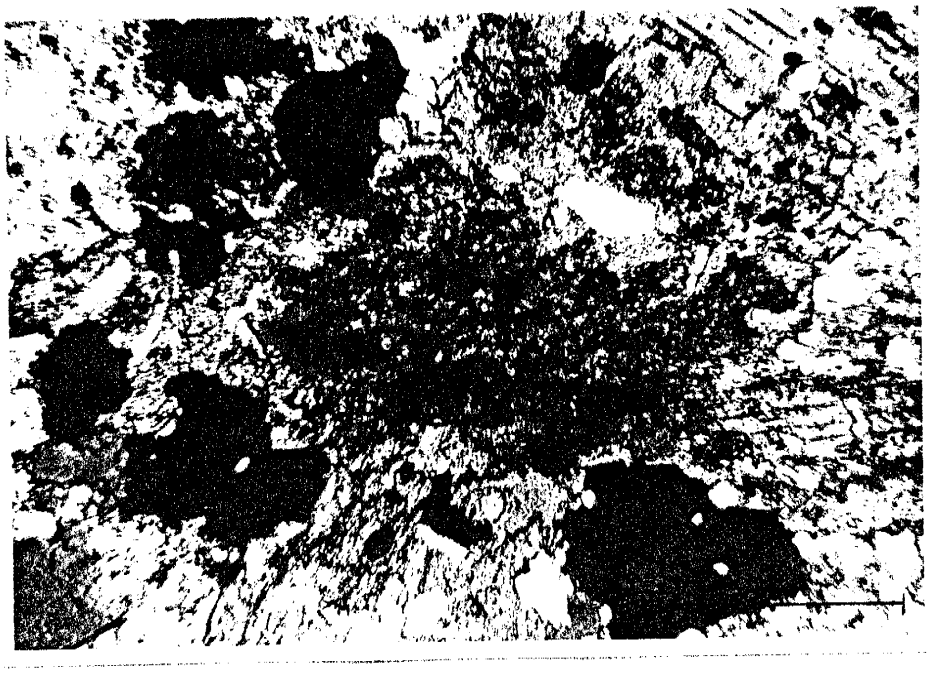

Figure 14b
Same as above (different thin section)
Black - magnetite, dark gray - hornblende, center - augite (Specimen D1)

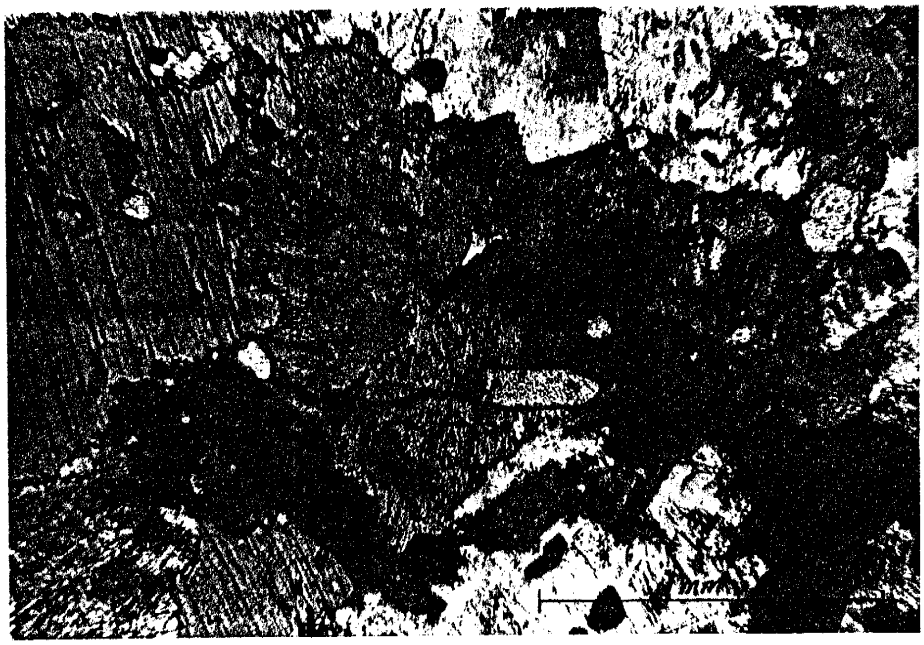

Figure 15a
Aggregate of hornblende grains with other mafics (Specimen H6) (plane polarized light)

Figure 15b
Interstitial hornblende - center (plane polarizred light) (Specimen E1)

common inclusions. Clustering with other mafics and accessories is typical. Interstitial hornblende is free of inclusions and has a fresh, unaltered appearance. It seems well distributed throughout the stock and shows a great variance in grain size. Judging from the somewhat mottled appearance of many grains of the two previous habits, it also occurs as a replacement.

Hornblende, with the exception of interstitial hornblende, is occasionally rimmed and replaced along cleavage cracks by biotite. Infrequently, hornblende is replaced internally and marginally by calcite. Alteration to epidote is commonly observed.

Diopsidic augite occurs most frequently as rounded to irregular relic cores enclosed in single crystals of hornblende. The boundary between core and rim is sharp with core diameters averaging 1 mm. Subhedral to anhedral, unaltered grains are uncommon. Single grains range from 0.7 mm to 1.5 mm in size. Augite is always accompanied by other mafics, plagioclase, and accessories among which it is usually centrally positioned.

Magnetite is the most abundant accessory mineral and is commonly allied with the dark minerals. Grains are irregular and as much as 0.5 mm across. Borders are often altered to hematite. Sphene is relatively abundant in every thin section and tends to partially bound magnetite or more probably ilmenite. Grains are irregular to subhedral and rarely euhedral. In thick sections, sphene is red-brown and

pleochroic. Occasionally grains are coated with leucoxene. Euhedral apatite is common with some grains up to 0.5 mm in length. Rounded zircons, 0.5 mm in maximum diameter, are widespread in small amounts. Allanite was found in about half of the thin sections studied as an accessory constituent.

STRUCTURAL CHARACTERISTICS

Contacts with Older Rocks

The external contact of the pluton has a variable dip, but in general dips outward at a steep to vertical angle on the eastern side and at a less steep dip along the southern end. The western margin is bounded by a vertical fault. The structural relationships are illustrated on Figure 16.

The contact with the Precambrian quartzite is sinuous to jagged in outline and is discordant. Quartzite along the southern contact has a variable strike and dip and has the appearance of having been mildly shouldered aside and wrapped around the stock in the manner as described by Noble (1952). The contact is well exposed here and is accompanied by a zone, approximately 15 feet wide, of quartzite inclusions which are oriented subparallel to the contact. Contact effects are feeble within this zone. The pluton has only a slight decrease in matrix size while the quartzite shows no obvious sign of contact metamorphism in outcrop. Small apophyses of granite are a common occurrence (fig. 17). Quartzite outcropping in the northeastern most corner of the stock has a steeper and more easterly dip and is in fault contact with the stock. Its attitude, however, suggests a relationship similar to that seen in quartzite along the southern border.

Figure 16

STRUCTURE MAP OF THE ANCHOR CANYON STOCK AND BORDER ROCKS

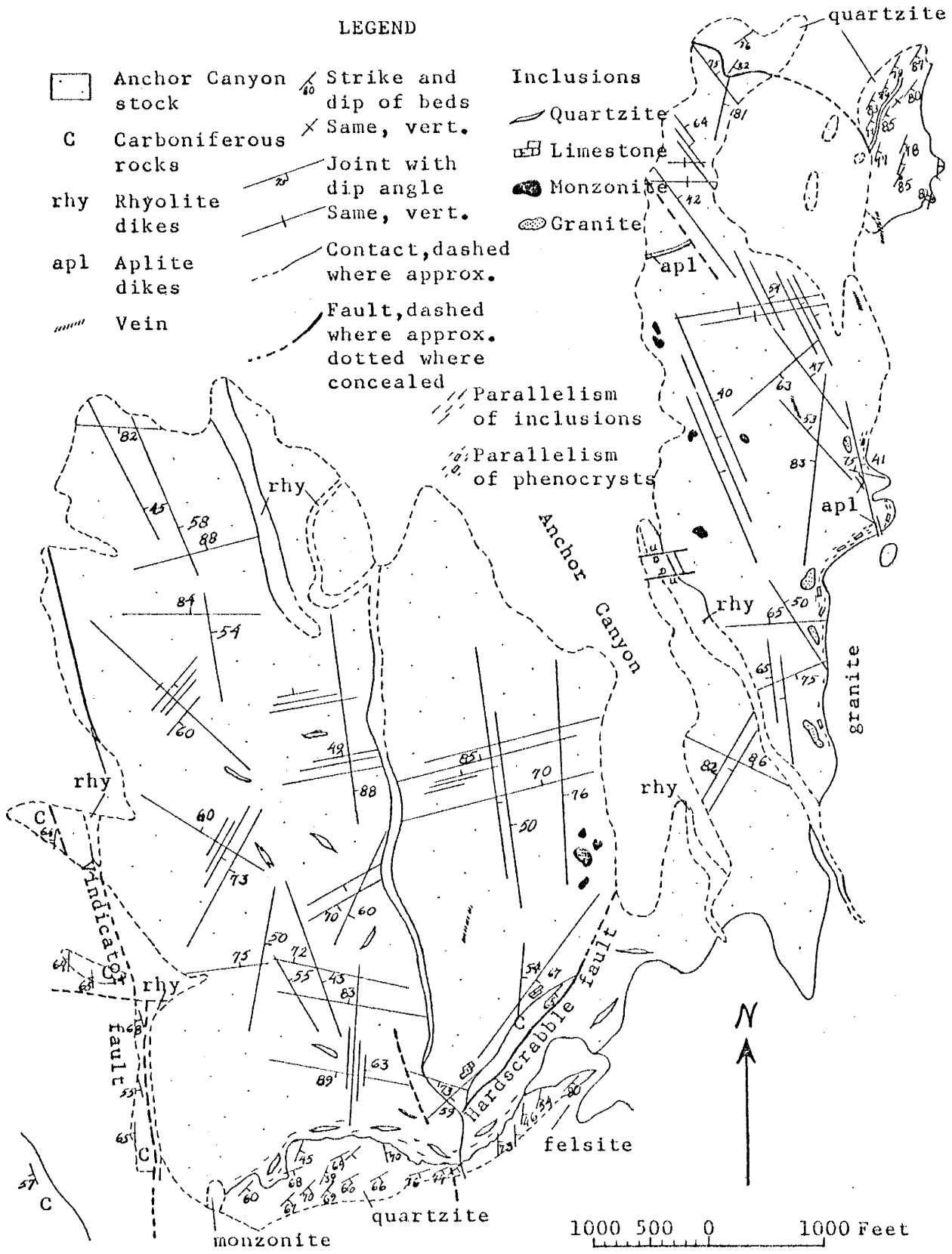

The eastern contact with Precambrian granite is lobate in appearance and outcrops poorly. Where exposed, the contact is sharp and, unlike the quartzite contact zone, is almost devoid of inclusions. The contact itself, with respect to the Tertiary pluton, is represented by a three to six inch wide layer of a fine-grained highly porphyritic facies with phenocrysts of plagioclase in strong parallel alinement with the border. This facies shows a rapid transition into the typical medium-grained porphyritic texture. The zone is easily weathered, most likely due to extreme crushing of the minerals. As with the quartzite, the Precambrian granite shows no apparent thermal effect. Apophyses of medium-grained Tertiary granite or quartz monzonite occasionally transect the border and contain xenoliths of Precambrian granite and diabase.

The western contact with Paleozoic sediments is discordant. The attitude of the Paleozoics south of the stock is similar except here their dip is between 15° and 20° greater than those farther to the south and may indicate some additional upward flexing of the rock resulting from either faulting or the intrusion of the Anchor Canyon stock, or both. The exact contact is not exposed in outcrop, but Paleozoic rock in the immediate vicinity is recrystallized, brecciated, and generally disturbed. Loughlin and Koschmann (1942) have indicated this zone to be a fault contact representing movement after intrusion of the stock and along which mineralizing solutions migrated. The contact is in part intruded by a rhyolite dike also showing evidence of deformation.

The contact with the large, lenticular inclusion of Paleozoic limestone everywhere shows some effects of movement probably due to slippage during consolidation of the pluton. Its southeast contact is bounded by a fault while its northwest contact is concordant. The limestone has been largely metamorphosed into a light gray, coarse-grained marble, with some beds replaced by garnet and others by wollastonite.

Internal Contacts

Contacts between each of the four rock types, as noted earlier, are gradational with each other; the transitions being of a nature as to make it impossible to plot the boundaries accurately without the aid of modal analyses.

Xenoliths

Inclusions of older rock are commonly seen near intrusive margins, but are scarce within the pluton. Xenoliths are of four types: quartzite, Precambrian granite, monzonite, and limestone.

Quartzite xenoliths are found predominantly along the southern border where they occur as elongate, angular forms. They range from well preserved fragments a foot or more in length near the contact to small shadowy remnants averaging two inches in length elsewhere in the stock. Most of these inclusions are of Precambrian quartzite, but some may be of Paleozoic sandstone.

Granitic inclusions are rare and found only in close proximity to the contact with Precambrian granite. They are usually elongated with rounded edges and average between one and two feet in length (fig. 18). Diabasic material is also found here as xenoliths but only where diabase dikes cut Precambrian granite.

Xenoliths of monzonitic to dioritic composition are common locally. They are typically unaltered and are round to oval in shape. A concentration of such clots occurs in a ravine at the upper end of Anchor Canyon and are as much as two feet in diameter. Similar accumulations, with clots somewhat smaller in size, occur in ravines on the east side of Anchor Canyon, where they are often found weathering out of the enclosing rock. The rounded or oval, rather than angular shape, suggests either that the monzonite had not become well solidified before it was invaded by the pluton or that the corners and edges of the fragments were resorbed by magma.

Limestone inclusions are not commonly seen and are restricted to the vicinity of the large block of Paleozoic limestone within the Anchor Canyon stock. They are typically irregular in shape with rounded edges and rarely exceed one foot in diameter. Many are almost completely incorporated into the surrounding rock making them difficult to recognize. One thin section from a sample taken near Hardscrabble mine had in it a small cluster of anhedral plagioclase grains and probably represents assimilation of Paleozoic rock.

Figure 17
Apophysis of granite into Precambrian quartzite along southern border

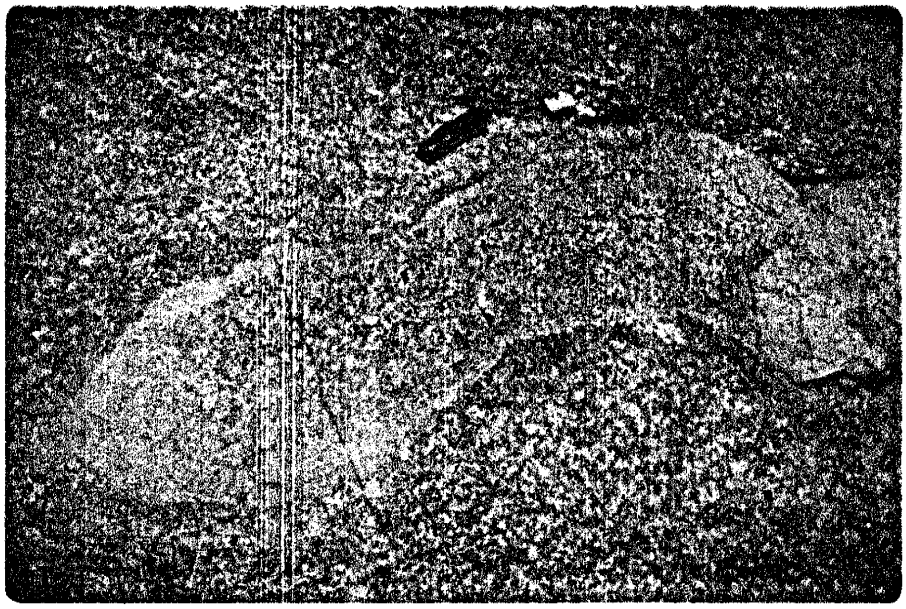

Figure 18
Inclusion of Precambrian granite near the eastern border

Flow Structures

Rock comprising the Anchor Canyon stock is generally massive. Parallelism of the quartzite inclusions along the southern border and of phenocrysts along the eastern border are the only useful planar structures. Less frequent is the alignment of biotite grains around inclusions of granite near the eastern border.

Faulting and Hydrothermal Veins

The Anchor Canyon stock has been subjected to recurrent regional disturbances along major fault zones probably developed earlier during Laramide time. Faults recognizable within the pluton are few. The largest fault is the Hardscrabble fault which lies along the southeastern contact of the large limestone inclusion. It strikes N. 30° E. and dips 60° to 70° S.E. and extends northward into Anchor Canyon where it is associated with hydrothermal pyritic veins, now altered to limonite. On the east side of Anchor Canyon two faults with a strike separation of 250 feet have faulted down a segment of a west-dipping white rhyolite dike forming a small graben. Further north, a northwest trending fault cuts off an aplite dike. A ridge near the southern border shows an apparent offset by a similar fault with a slightly more northerly trend and appears to extend on south into older rock.

The Vindicator fault, external to the pluton and largely concealed by alluvium, has a northerly trend and vertical to

steep easterly dip along the western boundary. It has been intruded by a white rhyolite dike and is associated with a sulfide vein. Two periods of movement can be detected, one before and one after the injection of dike material. Displacement along the fault cannot be determined directly, but if the Precambrian quartzite and felsite, just to the southeast, represents the surface upon which the basal unit of the Paleozoic was deposited, then the fault has dropped Carboniferous rocks on the west side at least 500 feet. This, however, does not take into account possible displacement by faulting prior to, and possibly obliterated by, the intrusion of the stock. An east-west trending fault which is buried by alluvium cuts the Vindicator fault. This fault was detected and mapped with the aid of a dip needle by Loughlin and Koschmann (1942).

Joints and Dikes

Major joint trends for the pluton are east-west, northwest, north-south, and northeast. Most joints are vertical to steeply dipping. Nearly flat-lying joints are also present, but were not recorded.

White rhyolite dikes have a north-south to north-west trend. They average 50 to 100 feet in width and thin southward where they finally pinch out a short distance beyond the southern border. At the terminus of the western ridge bordering Anchor Canyon, white rhyolite dikes thicken and have a less steep dip. The rhyolite is light gray and consists of quartz and orthoclase phenocrysts in a dense, felted

groundmass. The light coloring is a result of leaching solutions and weathering which left only minor portions of the dikes their original light brown color. Pyrite crystals altered to limonite are a common accessory. If north-northwest trending joints represent cross joints (Balk, 1937, p.27), then the white rhyolite may be a late differentiate genetically related to the stock.

Two aplite dikes with trends east-west and north-south occur along the eastern slope of Anchor Canyon. The aplite is light pinkish gray and fine-grained having the typical saccharoidal texture. Quartz and feldspar are the major components with biotite an accessory constituent.

MINERALOGICAL AND GEOCHEMICAL VARIATION

Mineralogical Variation

Mineralogical variation in the Anchor Canyon stock was studied principally by modal analysis of thin sections. In Figures 19-22, percent orthoclase, plagioclase, quartz and the volume percent of mafics + accessories, respectively, are contoured with a 5 percent contour interval. Since the pluton has high topographic relief, the 100 foot contours are shown on the isopleth maps and percent contours are drawn with some consideration given to the elevation differences between sampling localities. This method has been shown to be a better interpretation in areas of great relief (Whitten, 1961, p.242-243, 245, Peikert, 1965, p.333-335). In Figure 23, the mineral variations are plotted as functions of distance along section C-C' of Figure 3.

The mineralogical composition of the pluton varies systematically with elevation and in an east-west direction. The greatest rate of change, as seen in Figure 23, is the vertical direction. In the field, variations were recognized by noting changes in the content of dark minerals in conjunction with changes in average grain size and texture. Modal variation may be summarized as follows:

(1) Orthoclase shows the greatest over-all variability. Areas of high orthoclase content as shown in Figure 19

Figure 19. Variation of modal orthoclase. Data obtained by recalculating orthoclase, plagioclase, and quartz to 100 percent. Dots indicate sample localities.

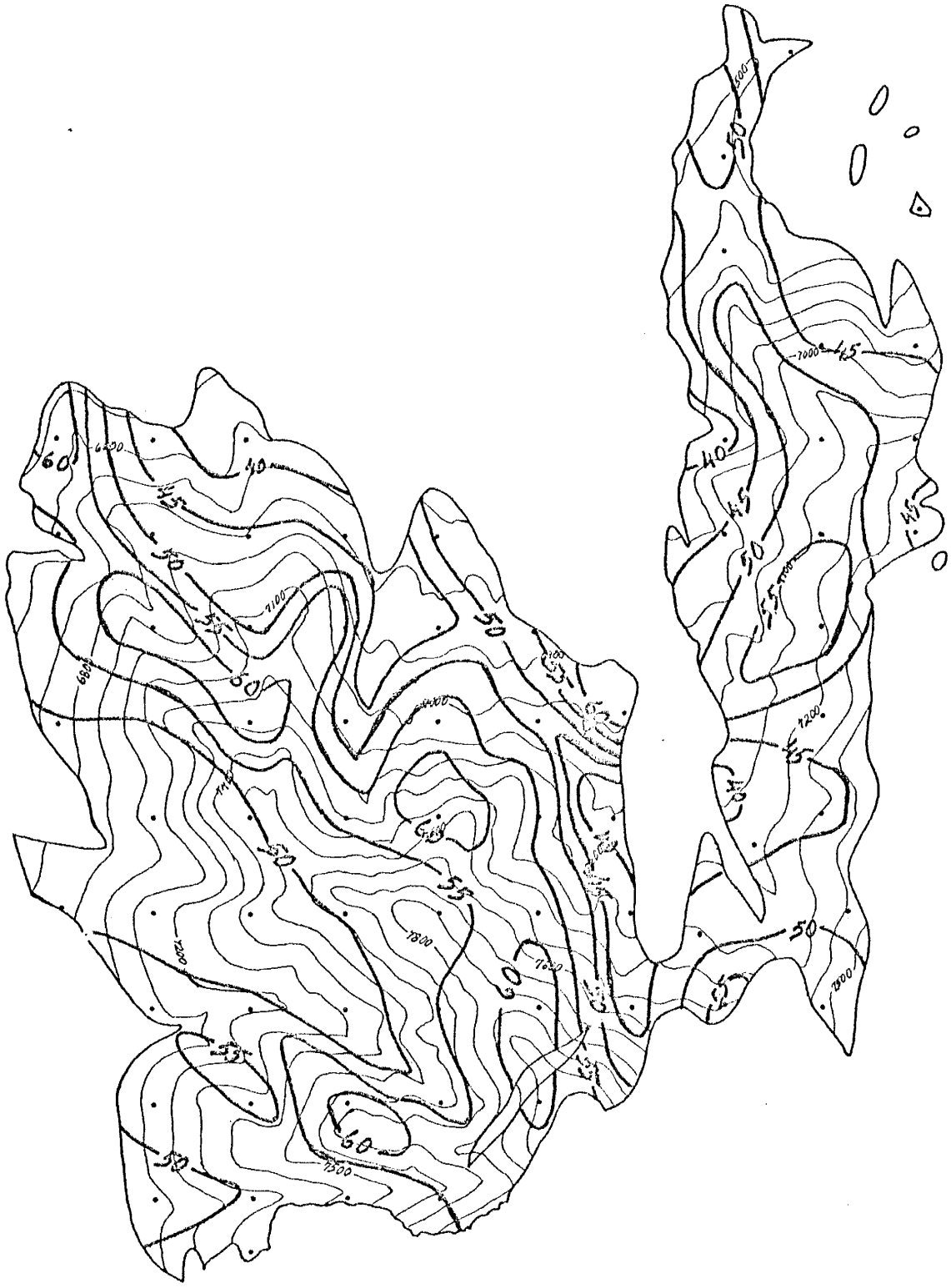

Figure 20. Variation of modal plagioclase. Data obtained by recalculating orthoclase, plagioclase, and quartz to 100 percent. Dots indicate sample localities.

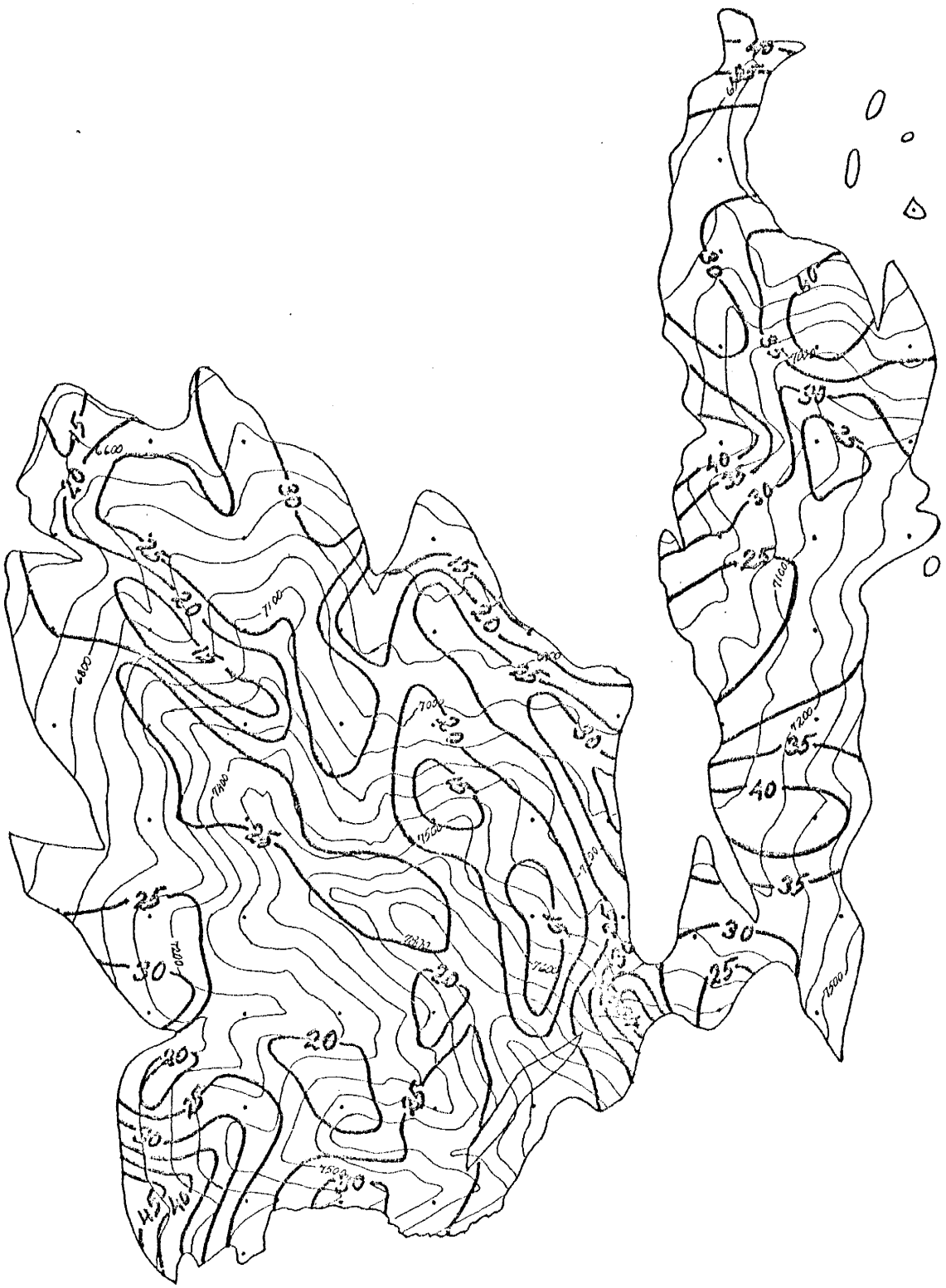

Figure 21. Variation of modal quartz. Data obtained by recalculating orthoclase, plagioclase, and quartz to 100 percent. Dots indicate sample localities.

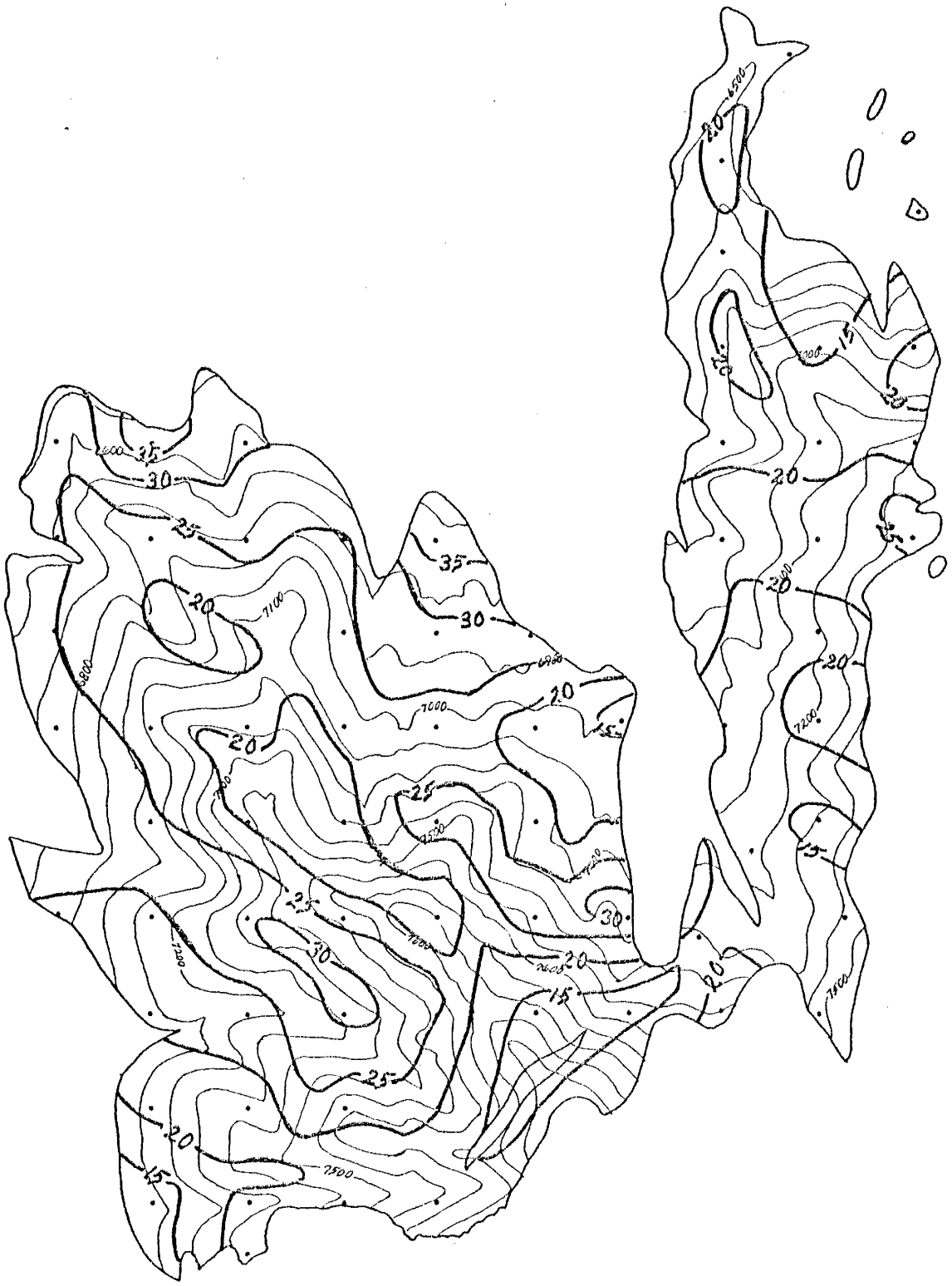

Figure 22. Variation of modal accessories and mafics. Data are in volume percent. Dots indicate sample localities.

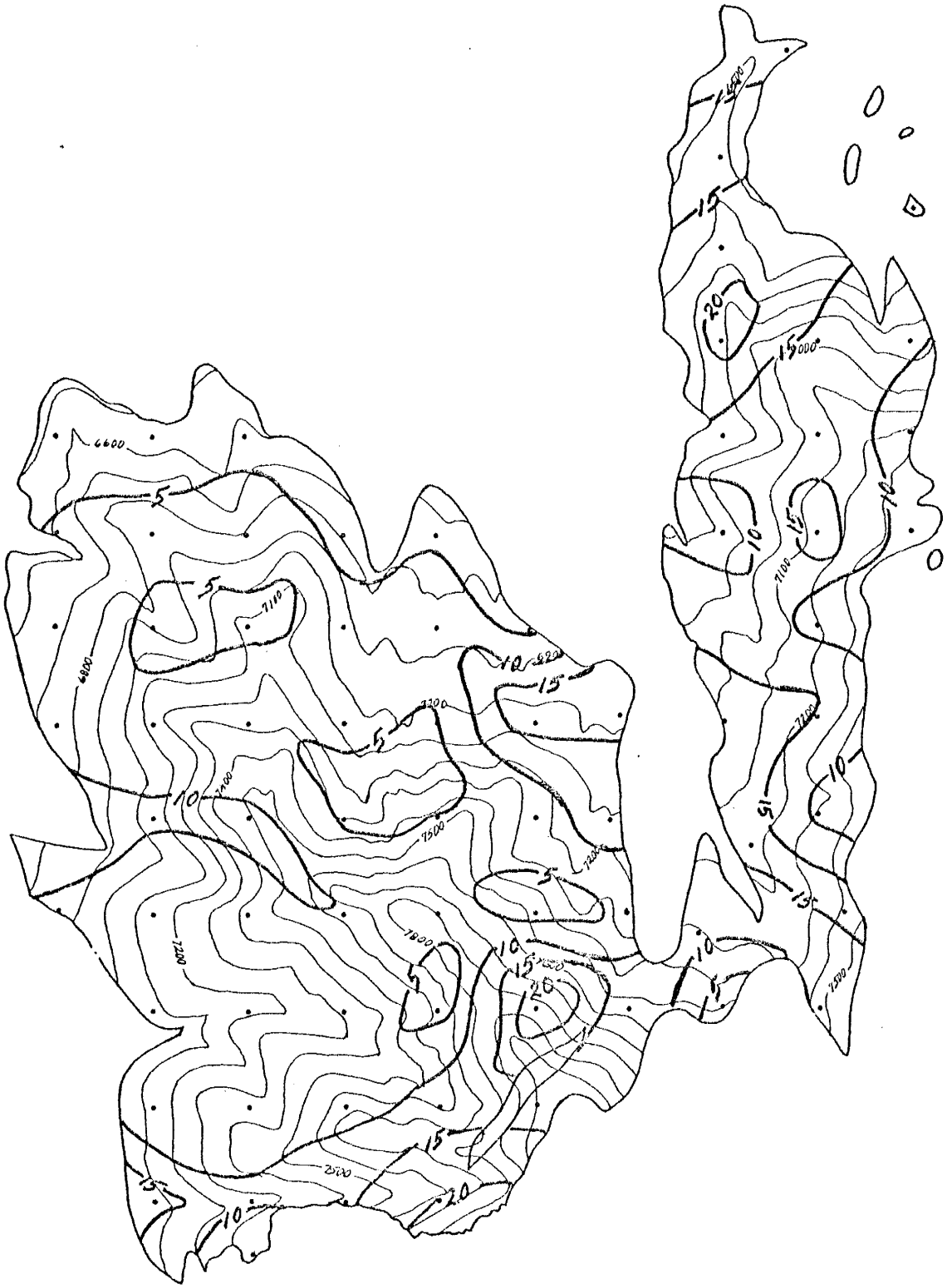

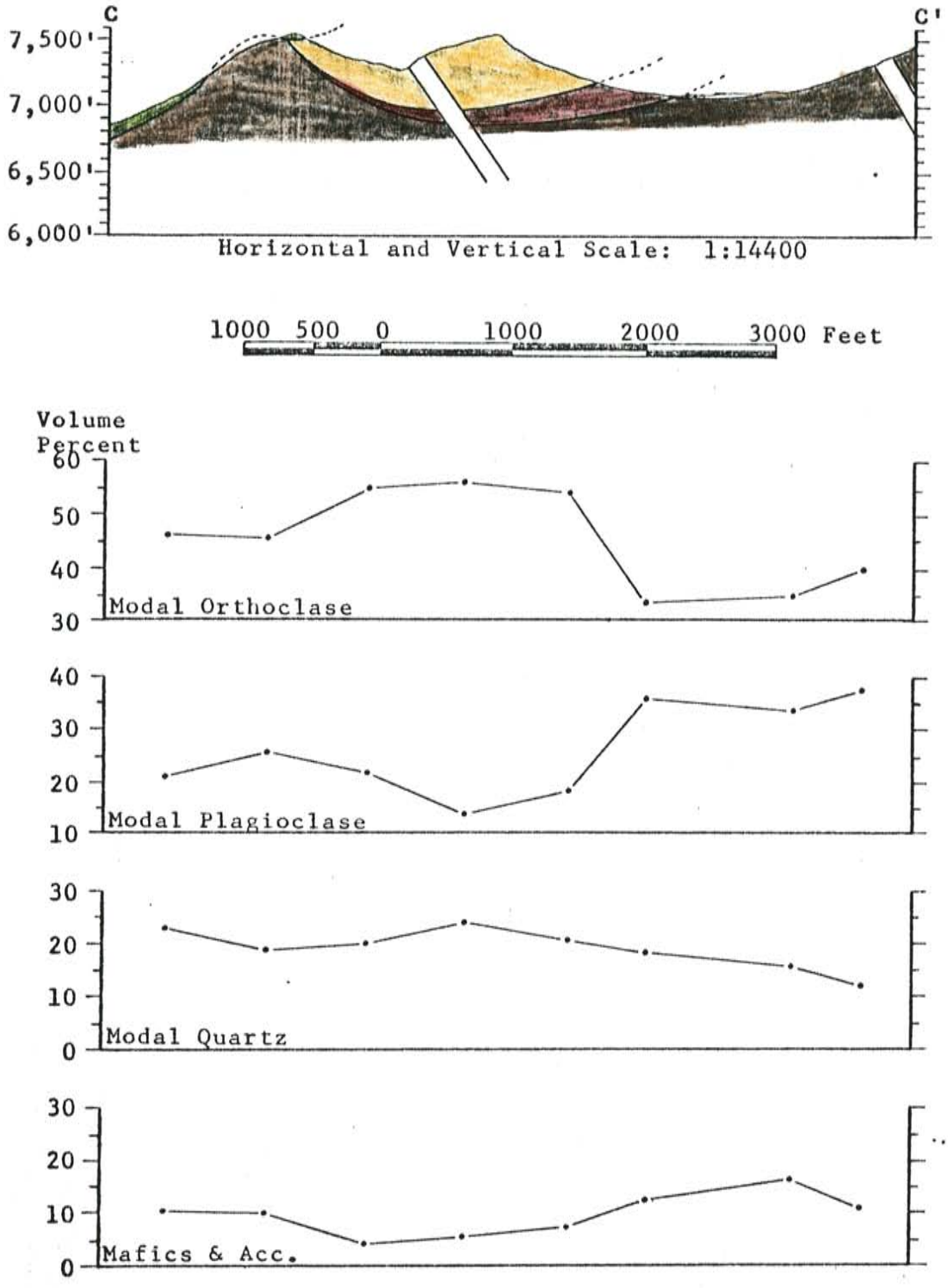

Figure 23. Cross section and mineral variation along line C - C' of Figure 3; brown: augite-quartz monzonite, red: hornblende-biotite-quartz monzonite, yellow-green: augite granite, yellow: hornblende-biotite granite.

occur on the western ridge and decrease with decreasing elevation except for one locality half way up Anchor Canyon. There is also a general increase in orthoclase westward across the stock.

(2) Plagioclase content (fig. 20) has a slightly smaller total variation and varies antipathetically with orthoclase.

(3) The variation in quartz may be large locally, but generally has a slow rate of change. Highest concentrations occur at the northern end of the western ridge while low concentrations, for the most part, are found on the southern and eastern margins (fig. 21). The vertical component of variation is still relatively large compared to horizontal variation. There is a vague correspondence between fluctuations in percent quartz and orthoclase.

(4) Total mafics + accessories, i.e. the color index (Shand, 1949, p.233), varies antipathetically with quartz, but shows a greater variation with relief (fig. 22). Excluding the high percentage shown at the southern border near the block of Paleozoic limestone, mafics and accessories decrease with rise in elevation and westward direction.

Modal quartz, alkali-feldspar and plagioclase (Table III) and normative quartz, orthoclase and plagioclase (albite plus anorthite) (Table IV) have been recalculated to 100 percent and plotted on a triangular quartz-orthoclase-plagioclase diagram

Figure 24. Plot of norms (listed on Table IV) and modes (listed on Table III), of granites and quartz monzonites from the Anchor Canyon stock. Arrows denote the trend in differentiation.

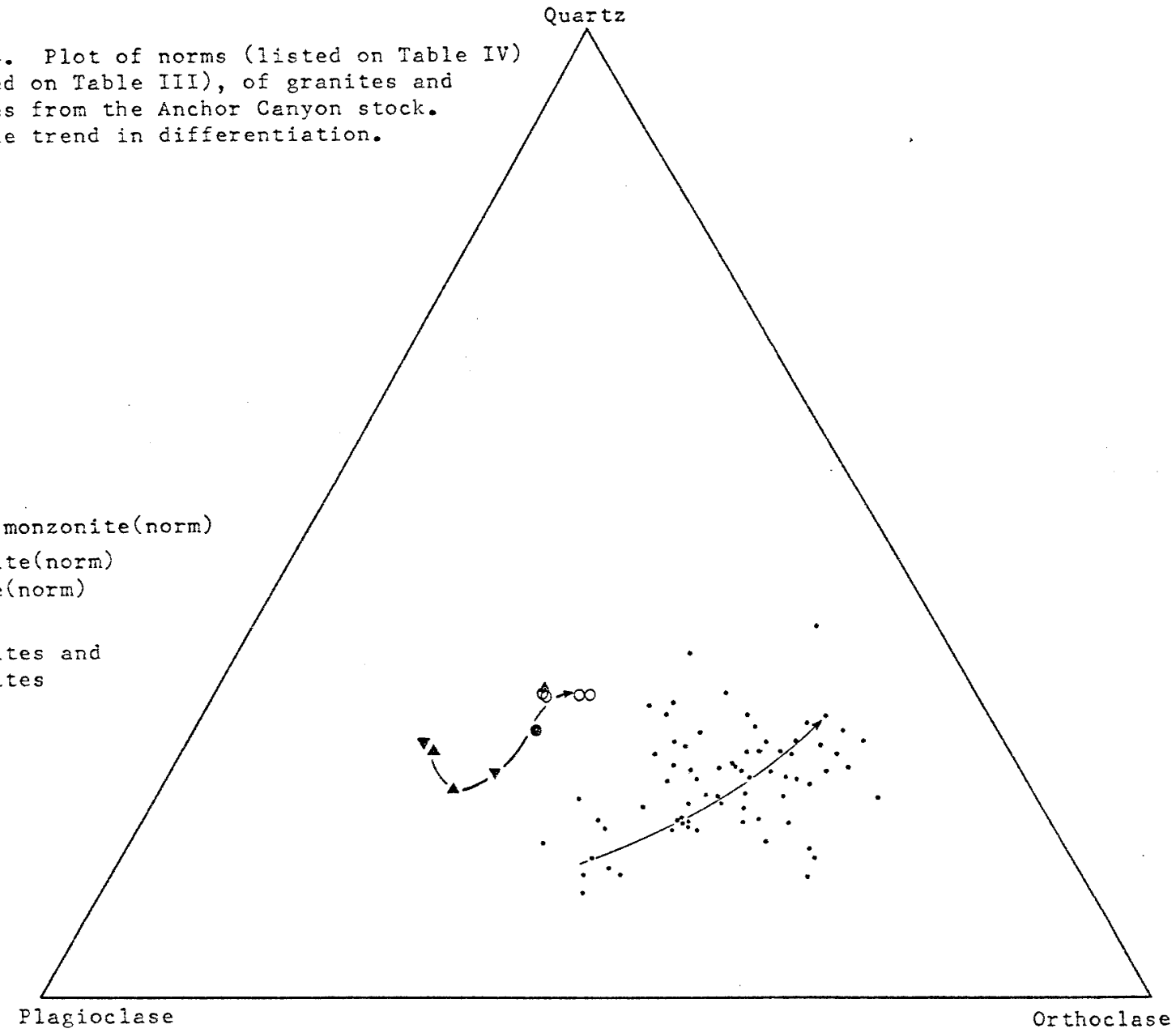

(fig. 24). On this diagram the modes fall in a broad band lying closest to the orthoclase corner while the norms plot in a curved line that extends from the center of the diagram toward the plagioclase corner. The different positions of the two fields is most likely due to the presence of albite in modal K-feldspar. The general trend in differentiation for both fields is indicated with an arrow.

Geochemical Variation

Ten rock samples, representing the range of rock types found in the Anchor Canyon stock, were selected for major and trace element analysis. The oxides of the major elements (Table IV) are plotted against silica in Figure 25; Figure 26 shows the relationship (A) between MgO, Fe_2O_3 (as total Fe) and (Na_2O + K_2O) and (B) between CaO, Na_2O, and K_2O on a triangular diagram (after Nockolds and Allen, 1953). Granitic rocks from the east-central Sierra Nevada (Bateman, et. al., 1963) representing a calc-alkaline trend; trachytic to rhyolitic rocks from Aden, southern Arabia (Cox, et. al., 1970), representing an alkaline trend; and andesitic rocks from Cape Nelson, eastern Papua (Jakes and Smith, 1970), representing a high-K, calc-alkaline trend, have also been plotted on Figure 26 for comparison. Graphs of copper versus silica and potassium versus strontium (fig. 27) were made to show the relationship between major and trace elements.

The SiO_2 content of the Anchor Canyon rocks range from 65.8 percent in quartz monzonite to 72.8 percent in granite.

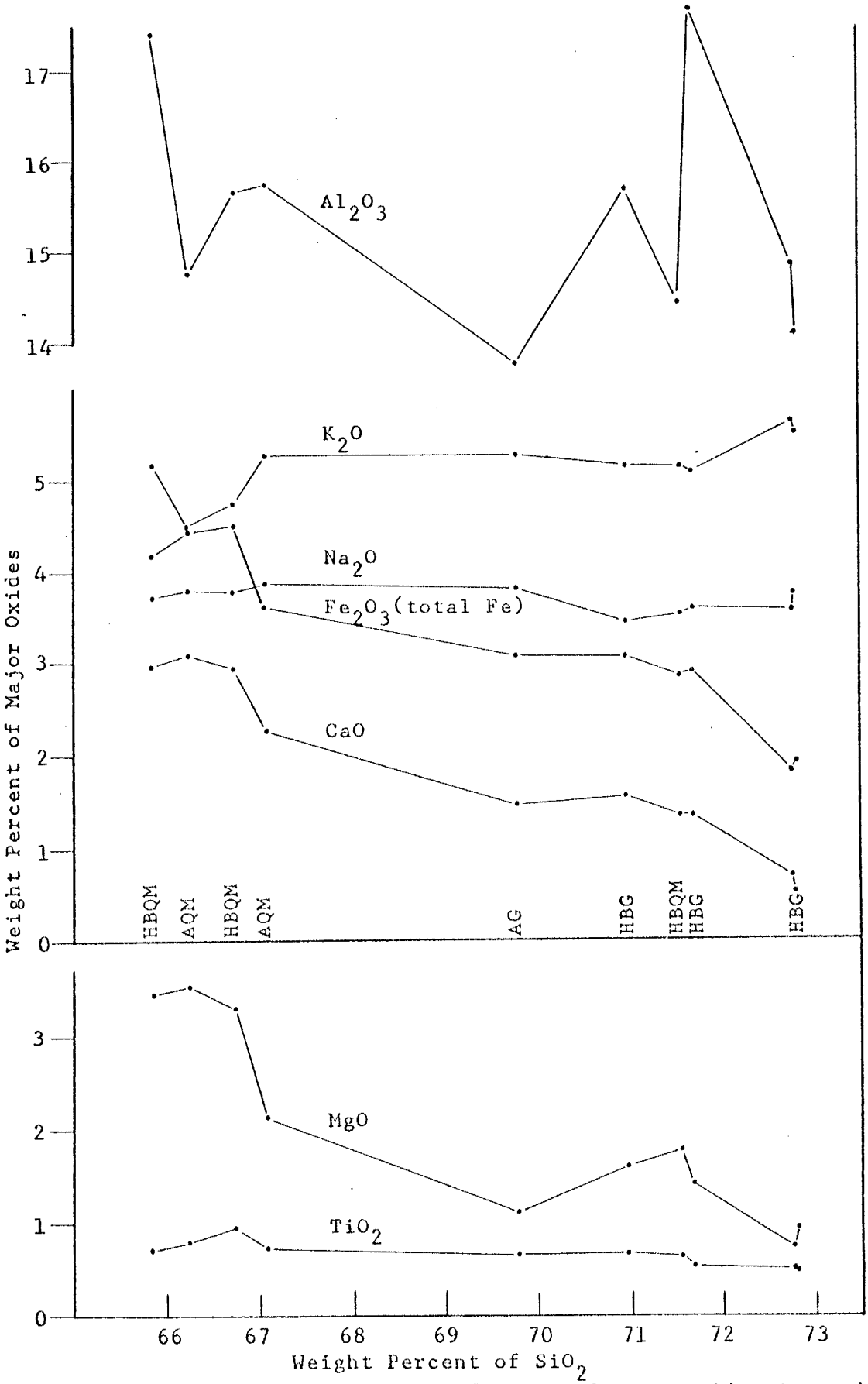

Figure 25. Variation diagram of major element oxides in rocks from the Anchor Canyon stock plotted against SiO_2.

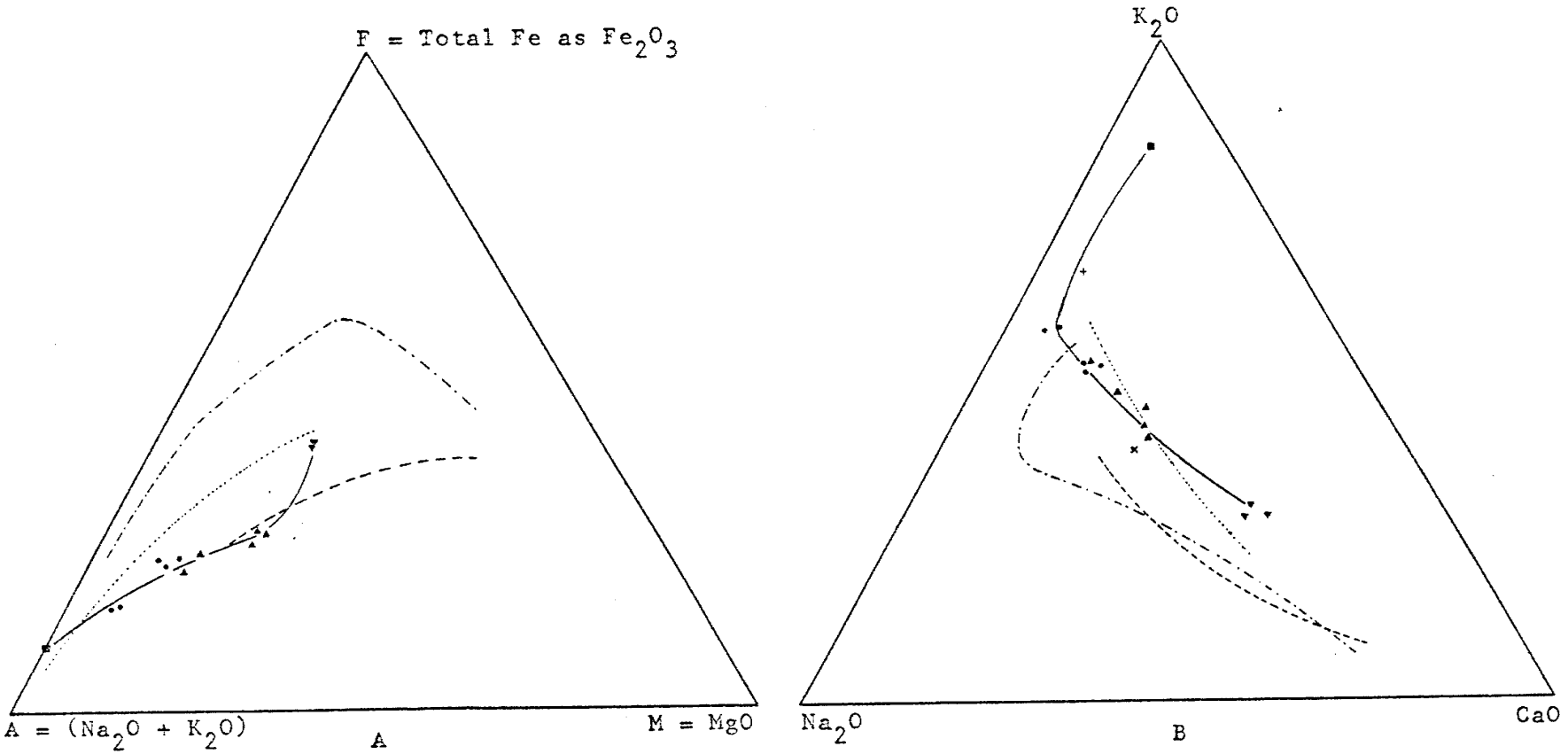

Symbols for Anchor Canyon and associated rocks:
- ▼ Monzonite(Loughlin & Koschmann, 1942, and Daly, 1914)
- ▲ Quartz monzonite
- • Granite
- × Quartz monzonite porphyry(Gordon, 1910)
- + Rhyolite porphyry(Loughlin & Koschmann, 1942)
- ▪ White rhyolite dike(Loughlin & Koschmann, 1942)

Figure 26. (A) AMF and (B) Na_2O-CaO-K_2O variation diagrams for rocks from the Anchor Canyon stock(solid line); for comparison the trend of calc-alkaline rocks from east-central Sierra Nevada (·····), peralkaline rocks from Aden(-·-·-), and high-K calc-alkaline rocks from Papua(----) are given.

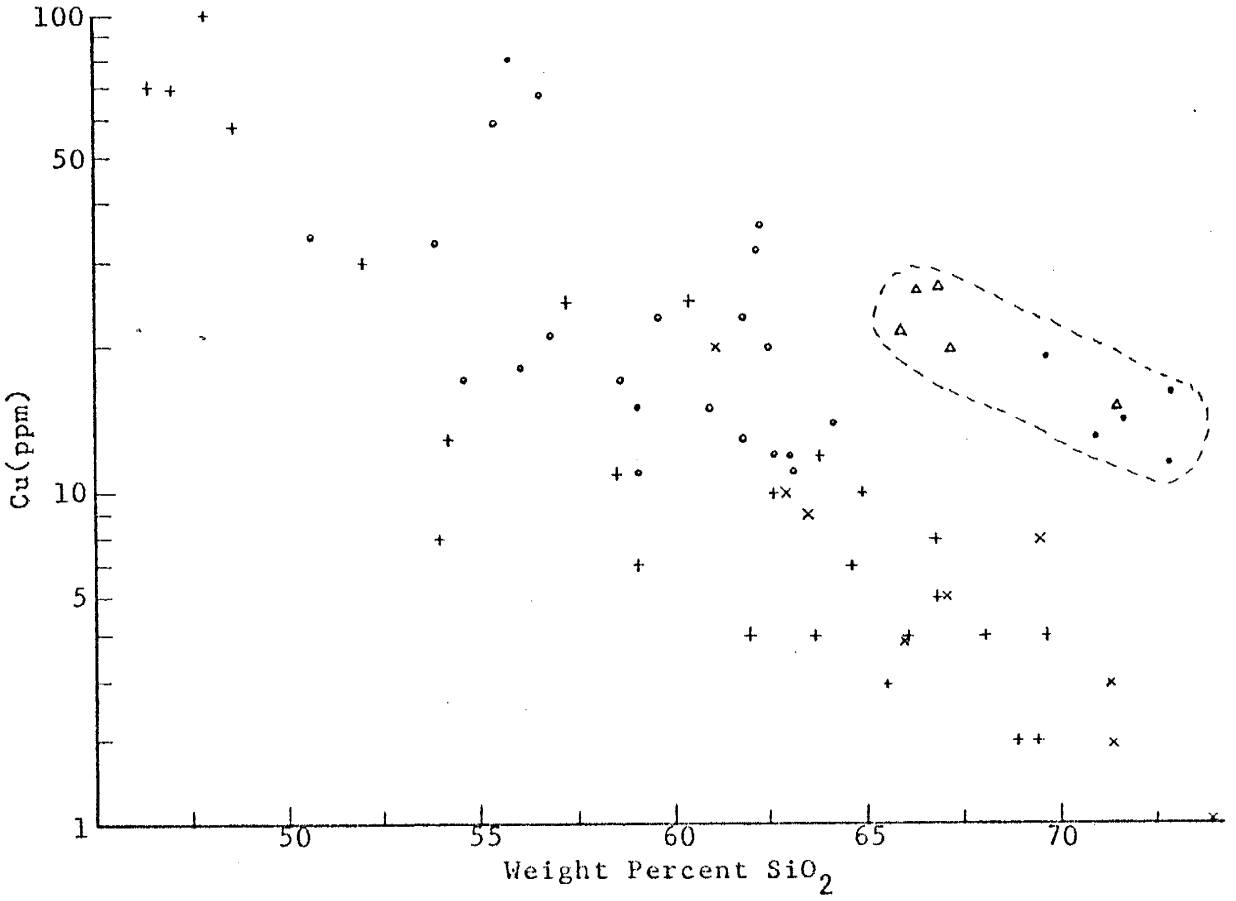

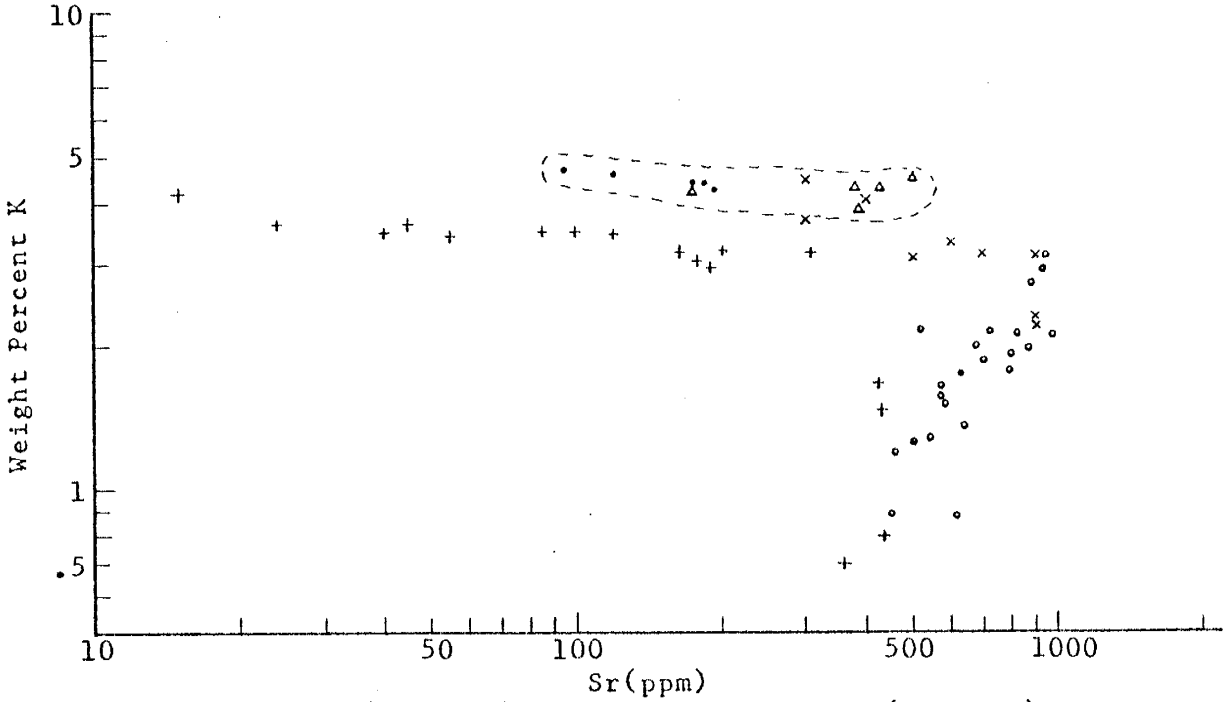

Figure 27. (a-above)Plot of Cu vs. SiO_2, (b-below)plot of K vs. Sr; triangles--Anchor Canyon quartz monzonite, dots--Anchor Canyon granite, crosses--granitic rocks from east-central Sierra Nevada, pluses--peralkaline rocks from Aden, circles--high K calc-alkaline rocks from Papua, (----)--field of Anchor Canyon rocks.

There is an apparent absence of rocks with silica percentages between 67.1 and 69.8, but this may not be real.

It can be seen from Figure 25 that as the silica content increases, Al_2O_3 varies widely; normally, there is a relatively uniform decrease of Al_2O_3 with increasing silica. This wide fluctuation, however, may be typical of high-K, calc-alkaline rocks (Jakes and Smith, p.265, 1970).

TiO_2, CaO, MgO, and Fe_2O_3 (as total Fe) are all regular in that they decrease with silica. K_2O, after an initial sharp decrease, increases rapidly to 67 percent SiO_2 and remains stable until 72 percent where it again begins to rise. Na_2O is steady throughout the silica range.

On an AMF diagram (fig. 26), the Anchor Canyon rocks fall below typical alkaline and calc-alkaline trends but coincide closely to the high-K calc-alkaline trend. The Na_2O-CaO-K_2O plot, however, does match well with that of a normal cal-alkaline trend.

The abundances of Rb, Ba, Cu, Ni, Zn, and Sr correlate with SiO_2 and K_2O and with mineralogical variations. In general, Rb and Ba values rise with increasing SiO_2 content and Cu, Ni, Zn and Sr values fall. Rb values (316-370 ppm) are unusual in that they show only slight variation with silica. In contrast, Sr (96-504 ppm) decreases rapidly with silica. Figure 27b (K/Sr) illustrates this point and includes other rock suites for comparison. A Cu versus SiO_2 plot (fig. 27a) is an example of the decrease in ferromagnesium trace elements with increasing silica. Cu and Zn concentrations (11.8-26.9

and 147-32 ppm respectively) appear to be slightly above average for rocks of similar composition whereas Ni (5.6-16.2 ppm) is closer to the average.

HISTORY OF CRYSTALLIZATION

Initial Assumptions

The Anchor Canyon stock was intruded after deposition of the Hells Mesa Formation (30.6 m.y., 32.1 m.y., 32.4 m.y.; Weber, 1971, p.37-42) and before extrusion of the La Jara Peak Andesite (23.8 m.y.; Chapin, 1971). The Nitt stock and other monzonitic stocks north of Magdalena intruded rocks as high as the middle Hells Mesa or within about 2,000 feet of the surface (Chapin, 1971). The Anchor Canyon stock, although closely related in space and time, does contain an inclusion of Paleozoic limestone not far removed from its original position indicating the local persistence of Paleozoics following the Larimide uplift. It is estimated that between 1,000 and 2,000 feet of Paleozoic and volcanic rock remained giving a range of between 3,000 and 4,000 feet of overburden. This corresponds to an emplacement in the epizone according to the classification by Buddington (1959, p.677), a fact that is also born out by the discordance of the contact and lack of foliate structures. Assuming an average density of 2.7 gm/cc, the pressure at this depth can be calculated by the equation $P=\rho gh$ to be approximately 250-325 bars. The graph developed by Piwinskii and Wyllie (1970, p.73), gives a temperature for the beginning of melting of 780-800°C for a quartz monzonite magma at this pressure. Other graphs for

granitic melts give equivalent or slightly higher temperatures (Tuttle and Bowen, 1958, p.122; Walton, 1955, p.14; Turner and Verhoogen, 1960, p.519; Winkler, 1965, p.168). The existence of wollastonite in the contact metamorphic zone around the Paleozoic limestone inclusion sets a minimum temperature at intrusion of 630°C (Winkler, 1965, p.29) provided that the fluid pressure was equal to the CO_2 pressure. The actual thickness of the overlying rock at the time of intrusion, however, is only approximately known because of uncertainties as to how much of the Paleozoics and/or Hells Mesa Formation was removed by erosion and by the fact that the Anchor Canyon stock is more deeply eroded and lacks contacts with the volcanic rocks.

In Figure 28-A, the normative compositions of Anchor Canyon rocks have been projected onto the four faces of the Or-Ab-An-Qz tetrahedron. The liquidus relations of the system Or-Ab-An-Qz-H_2O at 1,000 bars H_2O pressure are also shown (after Tuttle and Bowen, 1958, and James and Hamilton, 1969). When all four faces are taken into consideration, it becomes apparent that the norms trend from quartz monzonite to granite and in a direction approaching the temperature minimum for the system of 725°C. This is in fair agreement with the above calculated temperature range of 780-800°C. This difference, however, suggests that the estimated depth of intrusion may have been greater or possibly that an eruption at the surface removed the final liquid portion of the melt. The tetrahedron is shown in three-dimensional form in Figure 18-B.

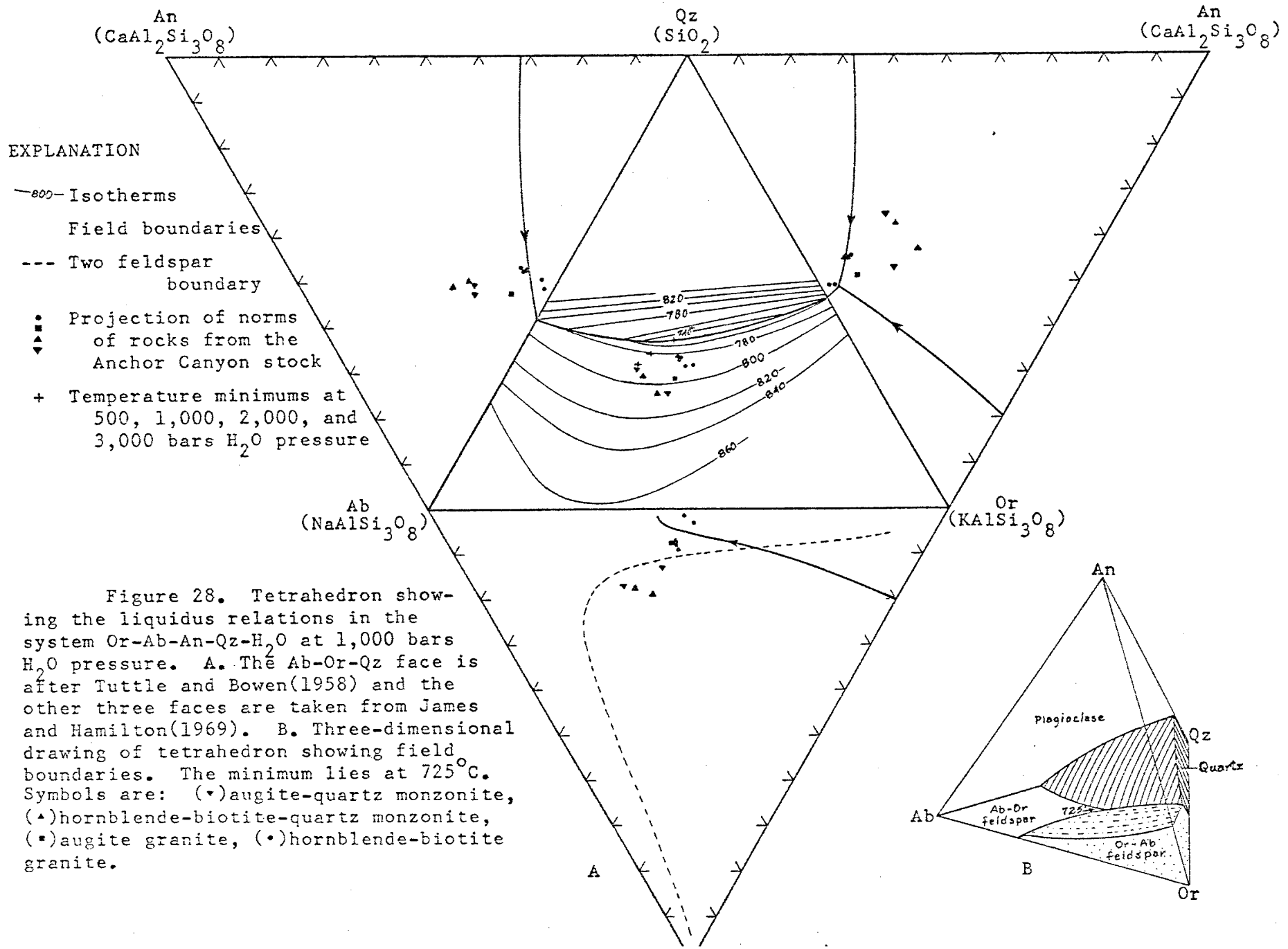

Figure 28. Tetrahedron showing the liquidus relations in the system Or-Ab-An-Qz-H_2O at 1,000 bars H_2O pressure. A. The Ab-Or-Qz face is after Tuttle and Bowen(1958) and the other three faces are taken from James and Hamilton(1969). B. Three-dimensional drawing of tetrahedron showing field boundaries. The minimum lies at 725°C. Symbols are: (▾)augite-quartz monzonite, (▴)hornblende-biotite-quartz monzonite, (▪)augite granite, (•)hornblende-biotite granite.

The composition of the melt at the time of emplacement would probably be best represented by an average of the modal data given in Table I for augite-quartz monzonite, since the other rock types are minor compared to the total volume of the pluton. This average composition is 47% alkali feldspar, 36% plagioclase, and 17% quartz. The normative average is 27% orthoclase, 48% plagioclase (Ab + An), and 25% quartz.

The following order of events in the crystallization history of the Anchor Canyon stock are based mainly on the foregoing assumptions, and on the experimental work of Piwinskii and Wyllie (1968), and on textural relations in conjunction with phase diagrams showing the stability fields of minerals.

Onset of Crystallization

Initial crystallization began with the formation of magnetite, then crystallization of diopsidic augite followed closely by labradorite. Ni, Cu, and Zn substituted for major elements in the crystal lattices of ferromagnesian minerals while Sr went into plagioclase. Accessories such as apatite, zircon, allanite, and sphene also formed about the same time. The composition of the melt alternated back and forth producing oscillatory zoning in the feldspar. This phenomenon may be explained in the following ways: (1) convection in a non-homogeneous magma, perhaps related to recurrent intrusion of magma from beneath an existing chamber (Wiebe, 1968, p.703); (2) recurrent incorporation of wall rock; (3) periodic

release of magma or/and volatiles into the upper crust resulting either in plutonism or volcanism. Vance (1962) discusses other less probable mechanisms.

As crystallization progressed, augite became unstable and began to react with the melt, subsequently being replaced by, or marginally altered to, hornblende. A further decrease in temperature enabled hornblende to crystallize directly from the melt followed shortly by biotite which, besides forming single crystals, also replaced hornblende and augite. Biotite may have preceeded hornblende in areas where conditions permitted. Nucleation of the later formed minerals generally took place on the surfaces of the earlier formed minerals because of the lesser energy required.

A sharp drop in pressure, presumably accompanying the ascent of the magma to a higher level in the earth's crust, caused partial resorption of plagioclase and hornblende, and eventually saturation in volatiles (Vance, 1962).

Main Stage of Crystallization

Continued rise of magma with decreasing solubility of volatile constituents, initiated rapid crystallization of minerals at many new sites and formed rims of sodic plagioclase around corroded plagioclase grains. Sodic plagioclase also sealed any holes in plagioclase developed during resorption, creating a patchy zoning as described and interpreted by Vance (1965). Turbulance, most likely associated with intrusive movement, left the magma well mixed and of homogenous

composition causing improved compositional correlation of outer plagioclase zones to each other and to matrix plagioclase (Wiebe, 1968, p.703). Normal zoning of plagioclase began and was characteristic of this period. Also, at this time, homogeneous orthoclase started to crystallize taking up rubidium which had concentrated in the melt. Concurrently, small amounts of quartz began crystallizing. Minor replacement of hornblende by biotite occurred. The bulk of the magma had solidified by the end of this stage.

Final Crystallization

This phase of consolidation was dominated by deuteric processes. Increased pressure resulting from the upward and inward concentration of volatiles was most likely attributable to fractional crystallization, reduced solubility and gravitational rise of volatiles, and early crystallization near the margins of the pluton (Jaeger, 1961, p.729-730) which rendered them impermeable. Crystallization proceeded more rapidly causing the simultaneous precipitation of orthoclase and quartz in graphic intergrowths (Deer, 1963, p.76). In close association came the mantling of orthoclase on plagioclase in areas of reduced volatile pressures (Stewart and Roseboom, 1962).

During this stage, unmixing of albite in orthoclase began. The remaining fluids, especially close to the roof of the intrusion, became relatively enriched in K_2O and SiO_2 presumably by volatile transfer. Na_2O remained constant.

A strong correlation between high quartz percentages and biotite exhibiting rutile inclusions (fig. 29) exists and is most likely the result of the concentration of volatiles and accompanying extreme pressures near the roof (Deer, 1962, v.5, p.37-38, Schwartz, 1958, p.172-173).

With a reduction in volatiles away from the borders and upward, the stability field for actinolitic hornblende was reached, initiating deposition of hornblende interstitially and as cavity fillings. Actinolitic hornblende is Mg-rich and is interpreted as resulting from the inability of the crystal lattice to accept aluminum at low temperatures (Harvy, 1950; Thompson, 1947; Engel and Engel, 1962, p.1512; and others cited by these authors).

Movement within the magma during the final stages of consolidation caused some crushing and straining of minerals particularly near intrusive margins.

Plagioclase deposition, which has been minor in this period, terminates and is followed later by interstitially deposited quartz and orthoclase. Unmixing of alkali feldspar to microperthite ceases on expulsion of the volatile constituents. Final crystallization apparently proceeded at a fast rate, otherwise, unmixing on a larger scale would have taken place (Tuttle and Bowen, 1958, p.50). Hornblende near the roof of the intrusion suffered resorption as water was expelled.

Figure 29. Distribution of biotite exhibiting rutile inclusions in the Anchor Canyon stock.

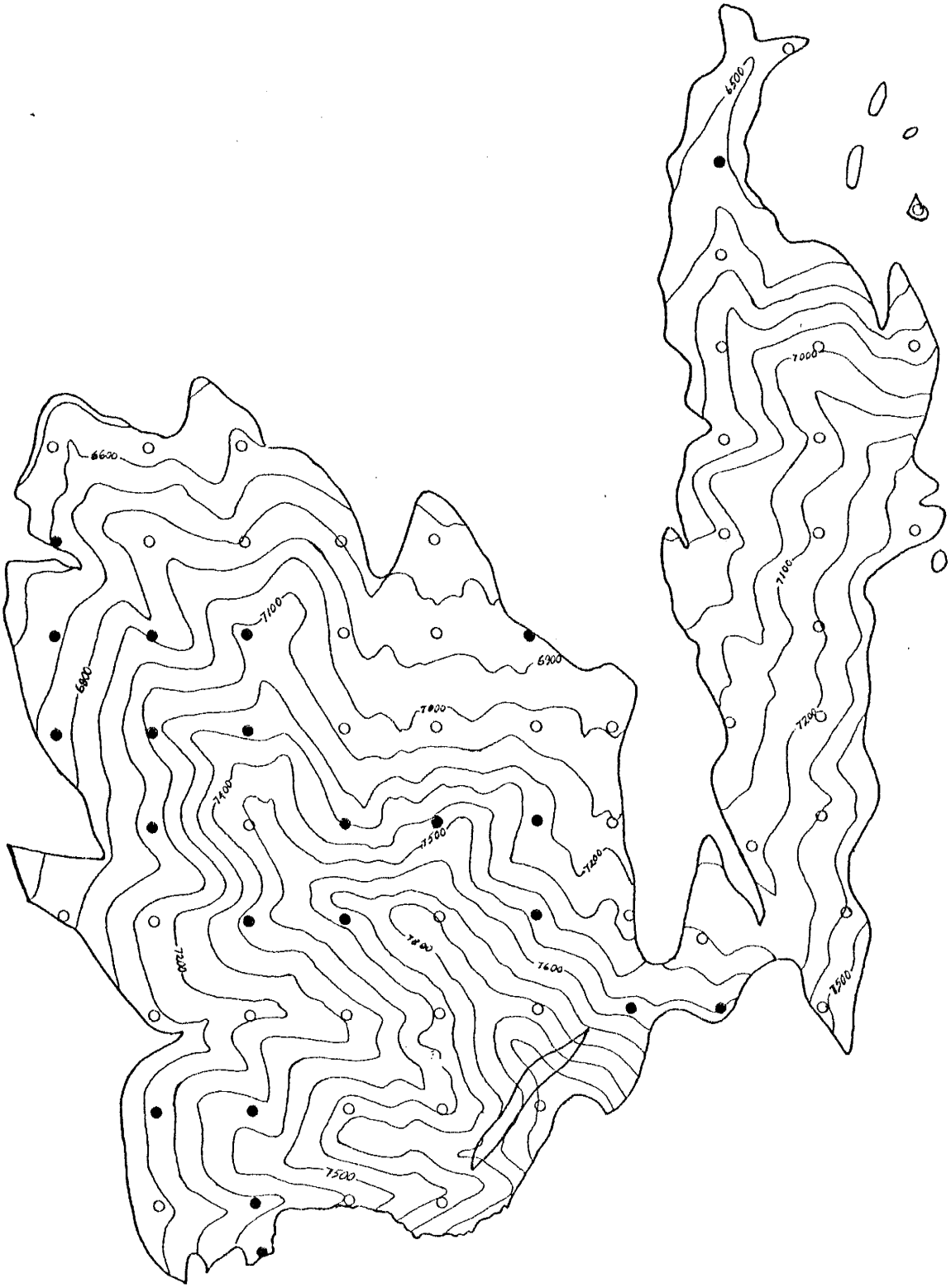

Late Stage Recrystallization and Alteration

Residual aqueous solutions became trapped in the upper part of the pluton during solidification giving rise to minor recrystallization. Recrystallized rock took the form of fine-grained irregular sheet-like bodies in rock of normal texture. Other fluids of unusual composition were also sealed off producing aplitic and pegmatitic material upon crystallization (Jahns, 1962). Gases also were caught up in the rock and formed miarolitic cavities. Minor amounts of myrmekite formed at the border of alkali feldspar.

Hydrothermal alteration occurred over a wide span of time ranging from late to post-magmatic. In general, solutions leached iron and magnesium, and substituted potassium, yielding secondary muscovite and sericite. Pyrite was deposited later in conjunction with mineralizing solutions affecting the entire district.

CONCLUSIONS

Cause of Mineralogical and Geochemical Variation

Before a discussion of the variation can take place, it must be pointed out that the Anchor Canyon stock has been uplifted and tilted westward. With this in mind, it can be assumed that the rock types occurring on the eastern side of Anchor Canyon have a lower intrusive horizon than those on the west side.

The basic concept of a steady rise and concentration of the volatile components in the uppermost part of the intrusion during solidification can be used to explain the major mineralogical and chemical variations within the Anchor Canyon stock. Volatile rise could have been accomplished in several ways. Convection and gravitational settling of ferromagnesian minerals and plagioclase may have displaced the liquid portion of the melt upward. The relatively larger percentage of mafic minerals and plagioclase phenocrysts in the rocks on the eastern side gives strong support to this mechanism. Geochemical evidence of this is seen in the decrease of CaO on Sr and other ferromagnesian trace elements with increasing SiO_2. Another means of separation could have been in response to a pressure gradient resulting from an eruption at the surface (Rutten, 1969). Early crystallized marginal portions of the pluton explain the migration of volatiles away from the

borders and also the existence of augite along the borders and at depth. Local dry areas may explain the preservation of minor augite not near the margins.

Assimilation of limestone by the magma though minor is seen by a sharp decrease in quartz content around the Paleozoic limestone inclusion. The reaction was characterized by the migration of silica and alumina into limestone inclusions leaving the magma depleted in these components and correspondingly enriched in alkalis. Evidence in the host rock for this transfer of ions are sedimentary beds replaced by wollastonite and garnet. Assimilation of Precambrian granite could help explain the patchy occurrence of more acidic rock on the eastern side of Anchor Canyon. Incorporation of monzonitic rock and quartzite, although it has taken place as shown by the modification of xenoliths, cannot be reconciled to have occurred on a large scale.

Origin and Mode of Emplacement

The present data do not permit a clear choice to be made for the origin of the Anchor Canyon stock. Three hypotheses for rocks having a calc-alkaline trend are consistent: (1) fractional crystallization of a primary basaltic magma, (2) partial melting of the upper mantle (Green and Ringwood, 1968), and (3) mixing of a mantle derived gabbroic magma with an anatectic granitic magma to form a melt of intermediate composition.

Piwinskii and Wyllie (1968) have emphasized the third possibility and show that magmas of such a composition would most likely be emplaced containing suspended crystals of plagioclase and hornblende or pyroxene where water is deficient.

A structural control for the intrusion of the Anchor Canyon stock is strongly suggested by its shape and location with respect to the Magdalena Range. According to Loughlin and Koschmann (1942, p.45, 57) there is evidence that the Nitt stock (monzonite) intruded a transverse fault zone and that the Anchor Canyon stock intruded along the axis of a mild flexure, most likely a northerly plunging anticline. More recently, Chapin (1971) has pointed out that these stocks were intruded along a major fault zone which trends N 10° W through the northern Magdalena Mountains and into the southern Bear Mountains. Since field relationships show monzonite to have been intruded by granite and ages on both stocks indicate a close association in time, it is reasonable to conclude that they are also genetically related. A strong point in favor of this is the striking resemblance between major mineral constituents of monzonite (Loughlin and Koschmann, p.36-39) and the earliest formed minerals found in rocks from Anchor Canyon.

With the evidence and assumptions given above, the following explanation of the evolution of the Anchor Canyon stock can be put forth. A reservoir of monzonitic magma in the lower crust was tapped as a result of faulting of the overlying rock, and ascent of magma formed the Nitt stock.

The parent magma continued differentiation until the composition of the remaining liquid became that of a quartz monzonite. The magma contained suspended crystals of calcic plagioclase, hornblende, biotite and to a lesser extent augite. At this time, another expulsion of magma triggered and guided by faulting occurred. The imbalance between magmatic pressure and resistance of roof permitted a passive injection of the magma characterized by the replacement of wallrock material with granitic melt by assimilation and digestion where possible. Where wallrock was of a high refractory nature stoping predominated. As the melt rose, presumably by its gravitational potential, the lighter fraction containing the volatiles partially separated from the heavier fraction and formed a thin capping on the upward moving column. Near the earth's surface, the crystal rich magma stoped into a fault zone causing only minor disturbance to the surrounding rocks.

Solidification began near the margins where an external corner provided the most rapid cooling surface (Jaeger, 1961, p.726), thus halting the reaction of augite crystals with the melt and preserving them as cores in aggregates of hornblende and biotite. Crystallization then proceeded inward with exsolved volatiles migrating inward and upward towards the already dome-shaped volatile-rich capping (Bowen, 1928, p.295-296). Convection and crystal settling also aided differentiation. The rocks, in general, became porphyritic due to the thinness of the roof (Kaguin, 1965).

With final solidification, the residual volatiles were driven off recrystallizing previously formed rock, creating sheet-like fine-grained variants (Karner, 1968, p.212), and metamorphosing the arched and overlying Paleozoic rocks to beds of marble and wollastonite. Joints developed perpendicular to the direction of greatest extension and some were filled with aplitic material (Balk, 1937, p.30) derived from trapped volatile constituents.

APPENDIX

Table I

Absolute Age Data
for the
Anchor Canyon and Nitt Stocks*

Sample	Location	Percent K	Percent Radiogenic Argon	Age (MY)
Tertiary intrusives				
8. Biotite from monzonite	Magdalena Nitt stock	7.55	41	28.0 (poor run)
9. Biotite from granite	Magdalena Anchor Canyon stock	7.40	51	28.3
			46	28.2

*R.H. Weber & W.A. Bassett (1963)

Table II. Characteristics of the Rock Types of the Anchor Canyon Stock

Rock Type	Texture	Orth.	Plag.	Quartz	Biotite	Hbld.	Other
I Augite quartz monzonite	Medium to fine grained porphyritic	35-45%	25-45%	10-25%	2-7%*	1-13%	1-4%
II Hornblende-biotite quartz monzonite	Medium to fine grained subporphyritic	30-45%	20-40%	15-35%	1-7%	0-10%	1-4%
III Augite granite	Medium grained porphyritic to fine grained subporphyritic	45-55%	15-20%	15-25%	3-6%	1-11%	2-4%
IV Hornblende-biotite granite	Fine grained subporphyritic	40-60%	10-25%	10-35%	1-7%	0-16%	1-6%

*augite included

Table III

Modal Data
Abundances Expressed as Volume Percentages

Specimen	Orth.	Plag.	Quartz	Biot	Hbld+Augite	Other[1]
A4	47.2	20.0	23.2	7.0	Trace	2.6
A6	46.5	19.6	25.5	4.2**	1.5	2.7
A7	50.9	18.2	22.9	5.5**	0	2.5
A8	51.3	19.3	24.0	3.1**	0	2.3
A9	58.8	12.0	25.6	2.1	0	1.5
B1	43.3	39.0	11.8	7.1	5.9*	2.9
B2	50.9	15.3	26.3	4.6**	Trace	2.9
B3	45.8	25.2	20.6	3.6	1.1	3.7
B4	46.9	23.6	22.5	5.0	0.3	1.7
B5	46.0	21.1	22.7	4.3**	2.5*	3.4
B6	48.2	23.3	21.8	3.7**	1.1	1.9
B7	61.6	13.3	19.6	3.0**	0	2.5
B8	44.9	27.5	21.2	4.3	0	2.1
B9	40.3	23.0	34.7	1.2	0	0.8
C0	48.3	19.5	24.5	3.8**	1.5*	2.4
C1	47.2	22.1	20.2	7.2**	0.5	2.8
C2	40.4	26.9	24.1	6.3**	0	2.3
C3	50.7	20.8	21.7	2.8	1.8	2.2
C4	45.1	19.8	26.6	3.8**	2.1	2.6
C5	45.7	25.6	18.7	5.0	1.9*	3.1
C6	56.2	13.9	22.0	4.8**	0.4	2.7
C7	47.1	28.0	19.8	3.4**	Trace	1.7
C8	42.4	24.9	25.2	3.9	1.1	2.5
C9	38.5	28.5	29.0	2.6	0	1.4

D1	42.3	28.0	15.0	3.5	8.3*	2.9
D2	55.1	16.0	21.9	2.4	2.3*	2.3
D3	42.7	20.7	29.1	4.5	0	3.0
D4	46.0	23.0	21.8	5.2**	1.7	2.3
D5	54.5	21.6	20.0	1.9**	0	2.0
D6	43.6	27.4	21.8	3.8	0	3.4
D7	53.8	15.3	24.6	4.4	0	1.9
D8	41.0	30.5	24.0	1.5	1.4	1.6
E1	44.4	20.7	14.6	5.4	11.3*	3.6
E2	44.8	24.8	17.5	2.2	7.5	3.1
E3	52.8	17.9	25.2	1.8	0	2.3
E4	50.0	24.9	18.2	4.1^{+}	0.4	2.4
E5	56.2	14.6	23.8	3.1**	0.2	2.1
E6	54.1	19.3	21.6	3.2	0	1.8
E7	38.2	26.1	26.5	4.6	2.3	2.4
E8	49.0	10.5	36.9	0.6^{+}	0	3.1
F2	54.3	20.3	13.4	0.2^{+}	7.7	4.2
F3	47.7	18.5	9.4	2.6	16.0	5.8
F4	56.4	13.2	26.5	2.6**	0	1.3
F5	54.0	18.3	20.3	5.0**	0	2.4
F6	40.9	27.5	15.0	4.5	9.8*	2.3
F7	53.7	13.9	27.6	2.7**	0.2*	1.9
G3	42.1	43.9	10.5	4.1**	7.3*	2.2
G4	39.4	25.9	28.2	4.3	0.8*	1.4
G5	33.4	36.1	18.1	3.2	6.8	2.4
G6	52.5	19.3	12.0	4.7	7.8*	3.7
H3	53.7	20.2	21.9	1.1‡**	0	3.1
H4	42.8	29.4	16.5	3.0	5.9*	2.6

H5	34.7	33.8	15.5	6.4	6.6	3.0
H6	44.4	22.5	14.7	4.7	10.5	3.2
H8	42.1	28.8	22.4	2.1	1.9*	2.8
H9	32.0	40.0	13.6	4.6	6.8	3.1
H10	39.7	23.1	15.7	7.5	10.3	3.7
H11	39.6	28.0	14.1	6.3	8.6*	3.4
H12	46.6	22.7	18.4	3.0**	6.5	2.8
I3	44.6	28.0	15.2	5.4	4.1*	2.7
I4	41.3	26.9	15.1	6.4	6.5*	3.8
I5	39.9	37.6	11.9	4.1	3.4*	3.1
I6	41.2	26.6	17.0	7.5	5.0*	2.7
I7	53.3	24.6	15.0	3.6	2.4	1.1
I8	41.3	22.5	19.9	6.6	7.0*	2.7
I9	52.0	20.8	15.9	5.8	3.8*	1.8
I10	36.2	36.8	12.3	5.3	7.6*	1.8
I13	35.0	33.2	14.4	3.1	13.5*	2.8
J8	41.4	26.3	23.8	3.0	3.2	2.3
J9	43.3	29.2	16.7	4.8	3.2*	2.8
J10	39.9	31.7	17.6	4.0	4.7*	2.1
J11	34.1	35.6	10.2	5.0	11.2*	3.9

* augite present

\+ biotite chloritized

** inclusions of rutile

1 magnetite, sphene, apatite epidote, zircon

Table IV. Chemical Composition of Granitic Rocks from the Anchor Canyon Stock

Sample No.	H5	I10	E2	J10	D2	B6	B3	B4	A8	A9
Major Elements (oxides, weight percent)										
SiO_2	65.8	66.2	66.7	67.1	69.8	71.0	71.6	71.7	72.8	72.8
TiO_2	0.709	0.800	0.936	0.714	0.686	0.673	0.643	0.525	0.532	0.490
Al_2O_3	16.9	14.8	15.6	15.7	13.8	15.7	14.5	17.7	13.9	14.2
Fe_2O_3*	4.17	4.44	4.50	3.61	3.10	3.10	2.88	2.92	1.88	1.96
MgO	3.45	3.53	3.30	2.13	1.22	1.60	1.79	1.41	0.75	0.92
CaO	2.96	3.09	2.94	2.28	1.49	1.58	1.40	1.38	0.72	0.55
Na_2O	3.72	3.80	3.78	3.87	3.83	3.46	3.55	3.62	3.60	3.78
K_2O	5.27	4.47	4.74	5.28	5.30	5.17	5.17	5.21	5.66	5.53
Trace Elements (ppm)										
Ba**	125	90	138	135	237	189	48	65	65	163
Cu	21.7	26.3	26.9	19.9	19.0	13.3	15.0	14.7	11.8	16.3
Ni	11.7	14.7	16.2	10.9	10.1	6.9	13.3	12.8	5.6	11.4
Rb	366	326	316	358	351	370	345	331	318	358
Sr	429	504	391	381	187	197	175	175	96	122
Zn	147	136	106	79	46	63	59	53	33	32
Barth Mesonorms										
Qz	18.2	21.5	21.2	20.2	24.6	28.1	28.7	28.4	29.0	28.7
Or	22.3	17.3	18.9	25.6	27.8	26.7	26.7	27.3	31.7	30.6
Ab	31.5	32.0	32.0	32.5	32.5	29.4	29.9	30.4	30.4	32.0
An	12.2	10.0	11.1	8.9	4.7	5.6	4.7	5.0	2.0	1.1
Bi	13.0	14.1	13.0	8.2	4.8	5.6	5.6	4.8	2.4	3.2
Mt	3.5	3.2	3.5	3.0	2.8	3.0	2.8	2.6	1.4	1.9
Sp	1.8	2.0	2.4	1.8	1.8	1.6	1.6	1.4	1.2	1.2
C	.6	.2	.2	.4	-	2.4	1.3	4.3	1.1	1.5
Hm	-	-	-	-	-	-	-	.3	.3	-
Wo	-	1.1	-	-	-	-	-	-	-	-

*Total Fe as Fe_2O_3
**Values approx. 6x too low

Table V. Optical Properties of Minerals of the Anchor Canyon Stock

Specimen	2V	Optic sign	Ext / Z:c	Pleochroism X	Y	Z
Augite						
B5	59.5°	(+)	40°			
E1	61.5°	(+)	41°			
E1	64.5°	(+)	44°			
G3	65.5°	(+)	43°			
Hornblende						
A6	85°	(-)	26°	pale green	pale yellowish green	light bluish green
B1	85°	(-)	26.5°	pale green	pale yellowish green	light bluish green
B5	85°	(-)	25°	pale green	pale yellowish green	light bluish green
C8	83.5°	(-)	23.5°	pale yellow-green	yellow-green	bluish green
E1	83°	(-)	23°	pale green	pale yellowish green	light bluish green
G3	85°	(-)	26°	pale yellow	pale yellowish green	light bluish green
H10	84°	(-)	23°	pale yellow	light green	light bluish green
J8	84°	(-)	23°	pale green	pale yellowish green	light bluish green
Biotite						
A6	0°	(-)		pale yellow	dark red-brown	dark red-brown
B1	0°	(-)		pale yellow	dark red-brown	dark red-brown
B5	0°	(-)		pale yellow	dark red-brown	dark red-brown
B8	0°	(-)		pale yellow	dark red-brown	dark red-brown
C8	29°	(-)		pale yellow-green	dark brownish green	dark brownish green
C8	28°	(-)		pale yellow	brownish green	brownish green
E1	0°	(-)		yellow	dark red-brown	dark red-brown
H10	0°	(-)		pale yellow	dark red-brown	dark red-brown
J8	0°	(-)		pale yellow	dark red-brown	dark red-brown
J8	15.5°	(-)		pale yellow	yellow green	yellow green
Orthoclase			X:a			
B8	59°	(-)	8.5°			
E1	62°	(-)	9°			
E1	71°	(-)	11°			
H10	59°	(-)				
H10	72°	(-)				

Table VI

X-Ray Diffraction Data from Powdered Alkali Feldspar Samples of Specimens B8 and H10

Reflection	2θ values for CuK_a radiation H10	B8
$(\bar{2}01)$	20.95	20.90
(002)	?	27.54
(131)	29.81	28.85
(222)	30.41	30.43
(041)	30.87	30.78
$(\bar{1}13)$	38.67	?
(060)	41.73	41.78
$(\bar{2}04)$	50.67	50.72

REFERENCES

Balk, R., 1937, Structural behavior of igneous rocks: Geol. Soc. America, Mem. 5, 117p.

Bateman, P. C., Clark, L. D., Huber, N. K. Moore, J. G. and Rinehart, C. D., 1963, The Sierra Nevada batholith: A synthesis of recent work across the central part: U.S.G.S. p.414-D, 46p.

Buddington, A. F., 1959, Granite emplacement with special reference to North America: Geol. Soc. America Bull., v.70, p.677-695.

Carrigy, M. A., and Mellon, G. B., 1964, Authigenic clay mineral cements in Cretaceous and Tertiary sandstones of Alberta: Jour. Sed. Petrology, v.34, p.461-472.

Chapin, C. E., 1971, K/Ar age of the La Jara Peak Andesite and its possible significance to mineral exploration in the Magdalena mining district: Isochron/West, in press.

Chayes, F., 1956, Petrographic modal analysis: New York, John Wiley & Sons, In., 113p.

Chayes, F., 1957, A provisional reclassification of granite: Geol. Mag., v.94, p.58-68.

Condie, K. C., 1967, Petrology of the late Precambrian trillite (?) association in northern Utah: Geol. Soc. America Bull., v.78, p.1317-1344.

Cox, K. G., Gass, I. G. and Mallick, D. I. J., 1970, The peralkaline volcanic suite of Aden and Little Aden, South Arabia: Jour. of Petrology, v.11, pp.433-61.

Daly, R. A., 1914, Igneous rocks and their origin: New York, McGraw-Hill Book Co., 563p.

Deer, W. A., Howie, R. A., and Zussman, J., 1962-1963, Rock-forming minerals: v.1-5, New York, John Wiley & Sons, Inc.

Emmons, R. C., 1943, The universal stage: Geol. Soc. America, Mem. 8, 205p.

Engel, A. E. J., and Engel, C. G., 1960, Progressive metamorphism and granitization of the major paragneiss, northwest Adirondack Mountains, New York: Pt. 2, Mineralogy: Geol. Soc. America Bull., v.71, p.1-58.

Engel, A. E. J., and Angel, C. G., 1962, Hornblendes formed during progressive metamorphism of amphiboles, northwestern Adirondack Mountains, New York: Geol. Soc. America, v.73, p.1499-1514.

Exley, C. S., 1963, Quantitative areal modal analysis of granitic complexes: a further contribution: Geol. Soc. America Bull., v.74, p.649-654.

Green, T. H., and Ringwood, A. E., 1968, Genesis of the calc-alkaline igneous rock suite: Contr. Mineral. and Petrol., v.18, p.105-162.

Harvy, W. T., 1950, Aluminum replacing silicon in some silicate lattices: Mineralog. Mag., v.27, p.142-149.

Hasofer, A. M., 1963, On the reliability of the point-counter method in petrography: Aust. J. Appl. Sci., v.14, p.168-179.

Jahns, R., and Burnham, C. W., 1962, Experimental studies of pegmatite genesis: a model for the crystallization of granitic pegmatites: Geol. Soc. America, Spec. Paper 68.

Jakes, P., and Smith, I. E., 1970, High potassium calc-alkaline rocks from Cape Nelson, eastern Papua: Contr.

Mineral. and Petrol., v.28, p.259-271.

James, R. S., and Hamilton, D. L., 1969, Phase relations in the system $NaAlSi_3O_5$ - $KAlSi_3O_8$ - $CaAl_2Si_2O_8$ - SiO_2 at 1 kilobar water vapour pressure; Contr. Mineral. and Petrol., v.21, p.111-141.

Johnson, J. T., 1955, A northern extension of the Magdalena Mining District: New Mexico Inst. Mining and Tech., unpublished master's thesis.

Kerr, P. F., 1959, Optical mineralogy: New York, McGraw-Hill Book Co., Inc., 442p.

Kottlowski, F. E., Weber, R. H., and Willard, M. E., 1969, Tertiary intrusive-volcanic-mineralization episodes in the New Mexico region (Disc.): Geol. Soc. America, Abstracts for 1969, Part 7, p.278-280.

Lasky, S. G., 1932, The ore deposits of Socorro County, New Mexico: New Mexico Sch. of Mines, State Bur. of Mines and Min. Res., Bull. 8, 139p.

Lindgren, W., Graton, L. C., and Gordon, C. H., 1910, The ore deposits of New Mexico: U. S. Geol. Survey, Prof. Paper 68, 348p.

Loughlin, G. F., and Koschmann, A. H., 1942, Geology and ore deposits of the Magdalena Mining District, New Mexico; U.S. Geol. Survey Prof. Paper 200, 168p.

Mackenzie, W. S., and Smith, J. V., 1956, The alkali feldspars III. An optical and X-ray study of high-temperature feldspars: Am. Mineralogist, v.41, p.405-427.

Noble, J. A., 1952, Evaluation of criteria for the forcible intrusion of magma: Jour. Geology, v.60, p.34-57.

Nockolds, S. R., and Allen, R., 1953, The geochemistry of some igneous rock series: Geochim. et Cosmochim. Acta, v.4, p.105-142.

Peacock, M. A., 1931, Classification of igneous rocks: Jour. Geology, v.39, p.54-67.

Peikert, E. W., 1965, Model for three-dimensional mineralogical variation in granitic plutons based on the Glen Alpine stock, Sierra Nevada, California: Geol. Soc. America Bull., v.76, p.331-348.

Piwinskii, A. J., and Wyllie, P. J., 1968, Experimental studies of igneous rock series: a zoned pluton in the Wallowa Batholith, Oregon: Jour. Geology, v.76, p.205-234.

Piwinskii, A. J., and Wyllie, P. J., 1968, Experimental studies of igneous rock series: felsic body suite from the Needle Point pluton, Wallows Batholith, Oregon: Jour. Geology, v.78, p.52-76.

Rutten, M. G., 1969, The ganggefolgschaft, a diagnostic feature to distinguish between plutons and rheoignimbritic pseudo-plutons: Geol. Soc. America Bull., v.80, p.545-548.

Schwartz, G. M., 1958, Alteration of biotite under mesothermal conditions: Econ. Geol., v.53, p.164-177.

Shand, S. J., 1949, Eruptive rocks: New York, John Wiley & Sons, Inc., 488p.

Smedes, Harry W., 1966, Geology and igneous petrology of the Northern Elkhorn Mountains Jefferson and Broadwater Counties, Montana: U.S. Geol. Survey, Prof. Paper 510, 116p.

Solomon, M., 1963, Counting and sampling errors in modal analysis by point counter: Jour. Petrology, v.4, p.367-382.

Stewart, D. B., and Roseboom, E. H. Jr., 1962, Lower temperature terminations of the three-phase region

plagioclase-alkali feldspar liquid, pt. 2: Jour. Petrology, v.3, p.280-315.

Thompson, J. B. Jr., 1947, Role of aluminum in the rock-forming silicates: Geol. Soc. America Bull., v.58, p.1232 (Abs.).

Travis, R. G., 1955, Classification of igneous rocks: Quarterly of the Colorado School of Mines, v.50, p.1-98.

Trȍger, W. E., 1959, Optische bestimmung der gesteinsbildenden Minerale, Teil 1 Bestimmungstabellen: Stuttgart, E. Schweizerbart'sche Verlagsbuchhandlung, 147p.

Turner, J. F., and Verhoogen, J., 1960, Igneous and metamorphic petrology: New York, McGraw-Hill Book Company, Inc., 694p.

Tuttle, O. F., 1952, Optical studies on alkali feldspars: Am. Jour. Sci., Bowen volume, p.553-567.

Tuttle, O. F., and Bowen, N. L., 1958, Origin of granite in the light of experimental studies in the system $NaAlSi_3O_8$-$KAlSi_3O_8$-SiO_2-H_2O: Geol. Soc. America Mem. 74, 153p.

Van der Plas, L., and Tobi, A. C., 1965, A chart for judging the reliability of point counting results: Am.

Jour. Sci., v.263, p.87-90.

Vance, J. A., 1962, Zoning in igneous plagioclase: normal and oscillatory zoning: Am. Jour. Sci., v.260, p.746-760.

_____ 1965, Zoning in igneous plagioclase: patchy zoning: Jour. Geology, v.73, p.636-651.

Walton, M., 1955, The emplacement of "granite": Am. Jour. Sci., v.253- p.14

Weber, R. H., 1971, K/Ar ages of Tertiary igneous rocks in central and western New Mexico: Isochron/West, no. 71-1, p.33-45.

Weber, R. H., and Bassett, W. A., 1963, K/Ar ages of Tertiary volcanic and intrusive rocks in Socorro, Catron, and Grant Counties, New Mexico: New Mexico Geological Society Fourteenth Field Conference, Socorro Region, p.220-223.

Whitten, E. H. T., 1961, Quantitative distribution of major trace components in rock masses: Am. Inst. Min. Metall. Engineers Trans., v.223, p.239-246.

Wiebe, R. A., 1968, Plagioclase stratigraphy: a record of magmatic conditions and events in a granite stock: Am. Jour. Sci., v.266, p.690-703.

Winchester, D. E., 1920, Geology of Alamosa Creek Valley, Socorro County, New Mexico: U.S. Geol. Survey Bull. 716-A.

Winkler, H. G. F., 1965, Petrogenesis of metamorphic rocks: New York, Springer-Verlag, Inc., 168p.

Wright, T. L., and Stewart, D. B., 1968, X-ray and optical study of alkali feldspar: I. Determination of composition and structural state from refined unit cell parameters and 2V: Am. Mineralogist, v.53, p.38-87.

Wright, T. L., 1968, X-ray and optical study of alkali feldspar: II. An X-ray method for determining the composition and structural state from measurement of 2θ values for three reflections: Am. Mineralogist, v.53, p.88-104.

This thesis is accepted on behalf of the faculty of the Institute by the following committee:

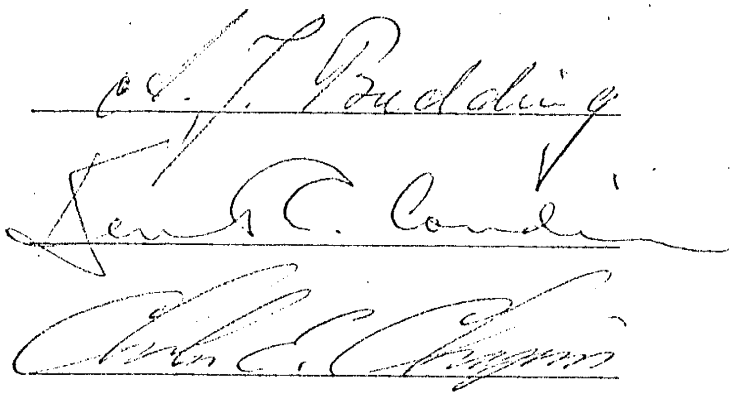

Date 5/6/71